Improving the Quality of Seed potatoes Using Precision Agriculture – Year 1 Report

1. Introduction

"Improving the quality of seed potatoes using Precision Agriculture" is a three year project looking at different ways of improving the quality of seed potatoes in New Zealand. Post desiccation re-greening is a major problem for our seed growers, along with controlling virus and CLso infected tubers. Both are costly to the seed grower and the latter has a flow on effect on yield and quality of ware crops.

After an initial project team meeting it was decided that in year one we would look at three aspects of desiccation management:

1. Seed potato cultivars differ in their ability for the tops to be killed by chemical desiccation. Due to re-greening after desiccation growers are often using 3-5 herbicide applications to try and remove growth and stop the tubers from growing. Therefore the first part of the project was to investigate the ability to use sensors and Precision Agriculture to detect regreening. This would allow subsequent targeting of control measures to treat those parts of the paddock differentially.

2. Investigate the effect of different water rates on efficacy of desiccation. Four water rates (200 L/ha, 250L/ha, 300L/ha and 400L/ha) and two different types of spray nozzles (Syngenta Defy and Syngenta Potato) within each water rate were evaluated for their effect on desiccation.

3. Investigate the ability to detect disease and virus using Unmanned Aerial Vehicle (UAV) technologies. Seed growers aim to minimise the chance for disease transfer (viruses and *Candidatus* Liberbacter solanacearum (CLso)) in infected potato seed tubers through rogueing and inspections. Being able to utilise PA through the use of UAV's could help seed growers improve seed quality by accurately targeting infected areas and minimising rogueing and inspection costs.

2. Materials and Methods

2.1 Using Precision Agriculture tools to detect re greening following desiccation

The paddock chosen was located on Accommodation Road near Methven in Mid Canterbury, South Island, New Zealand. The variety used was Moonlight, a main crop seed variety.

A DJI Phantom 4 Pro UAV with a 20 megapixel RGB camera was flown over the paddockon 23 February 2018, one day before application of the desiccant Reglone. Application occurred on 24 February 2018 and four drone flights were undertaken 3, 6, 9 and 16 days post application (27 Feb, 2 March, 5 March and 12 March respectively) to identify areas of green foliage. Each flight was undertaken using the DroneDeploy application, which involves taking geo-referenced photographs directly down on the crop, then stitching these images together to provide a high-resolution image of the crop.
6 plots of 3 beds wide by 20 plants long (2.6 x 6 metres) were marked throughout the paddock for assessment purposes, and coordinates recorded. Plant & Food Research (PFR) were contracted to carry out assessments pre and post initial application, however due to issues with technology only one assessment was carried out on 7 March 2018. Each plot was assessed by PFR with every plant in those plots assessed for the incidence of disease and virus along with the level of green leaves.

Using the Normalised Difference Vegetation Index (NDVI) tool in DroneDeploy, data from the images was used to visually identify areas with different intensity of green colour. When areas of interest were identified 5 GPS points were generated (3 x coordinates for "green" areas, 2 x coordinates for "brown" coloured areas, which were assumed to be desiccated, and sent to PFR who were contracted to undertake in field ground truthing. If PFR identified any plants or areas of the paddock that exhibited visual difference to surrounding plants or areas while ground truthing they logged their coordinates to allow geospatial linking to the UAV maps.

2.2 Desiccation water rates and nozzles

A commercial scale trial was set up on Urrall Road in Mid Canterbury, to look at both water rates and spray nozzles and their subsequent effect on desiccation of potato haulm with the cultivar Agria. The trial was established after the project team had concerns with the water rates being used by growers (commonly 200-300L/ha of water). It was thought that higher the water rate the more effective the desiccation. Eight treatments were applied using a commercial grower's sprayer. Four water rates of 400L/ha, 300L/ha, 250L/ha and 200L/ha were applied with industry standard desiccant Reglone® (Diquat). There were three desiccation timings of 13, 23 February and 12 March. At each timing 2L/ha of Reglone® was used. At each water rate two spray nozzles were used, either a Syngenta Potato Nozzle or a Syngenta Defy Nozzle. The pressure used was2.5-3 Bar. The potato nozzles were placed on one half of the boom with the Defy nozzles on the other meaning treatments were half a boom width/tram width wide. The potato nozzle has a 30 degree angle where the Defy has a 38 degree angle with courser droplets. Both are designed to reduce drift (potato by 50% and Defy by 75%) and alternative forward and backwards. The length of the treatments were the length of the paddock, about 700m.

Within each treatment three assessment points were spatially marked down the tramline/treatment and used as reference points for multiple assessments. These assessment plots were 5m x 5m. Initial desiccation was on the 13th February 2018. Visual scores of % kill (out of 100) were taken at these three points 3, 10, 14, 17, 20 and 24 days post initial desiccation (16 Feb, 23 Feb, 27 Feb, 2 March, 5 March, 9 March and 13 respectively).

2.3 Ability to detect disease and virus using UAV

From crop emergence two sites were flown with a DJI Phantom 4 Pro UAV with 20 megapixel RGB camera. The sites were late planted (cultivar Agria planted 16-18 December) to ensure the likelihood of disease later in the season. Both sites 1 & 2 were located on the Rakaia Barrhill Methven Road, in Canterbury.

The UAV was flown over the crop approximately every 7 days commencing on 25 January 2018 at crop canopy closure until crop desiccation on 8 March 2018. Using the DroneDeploy tool, data from the images was used to classify areas larger than about 30x30m with different characteristics. These differences were identified by purely visually assessing the RGB image, as well as using DroneDeploy tools of NDVI to help identify areas, however there were only small ranges in the NDVI values. When areas of interest were identified 10 GPS points were generated; 5 x coordinates for "healthy" areas, 5x coordinates for "subject" areas. "Healthy" areas were categorised as the areas of the crop canopy that had the highest NDVI readings, while "subject" areas were areas of the crop canopy with the lowest NDVI values, see Appendix 6.1. These were sent to PFR who were contracted to undertake in field disease and virus identification and ground truthing. Any areas of interest identified by PFR when ground truthing were also logged for linking to the UAV maps. Note that the NDVI values of healthy crops vary even without disease, and therefore differences in NDVI may not indicate disease incidence.

The work was undertaken to see if a simple RGB camera on a UAV could identify zones of disease in the crop before it was visible to the naked eye without individual plant inspection. If not, additional sensing technology could be used. If there were differences in the crop canopy identified by the UAV image that were not visible to the naked eye, the GPS coordinates would then be ground-truthed by PFR to see if individual plant inspection would identify disease symptoms.

Assessments were undertaken by PFR on 7 and 8 March, 2018. At the 10 GPS points generated on the UAV images, plants were assessed for disease, virus, stress or any other visible symptoms to correlate with the UAV maps. Weekly UAV maps have been analysed and linked to GPS points of interest data when collected by PFR while ground truthing.

3. Results

3.1 Using Precision Agriculture tools to detect re greening following desiccation

Five drone flights to secure aerial images of the whole paddock were made at this site from one day before the application of desiccant to 16 days after the first application (27 February, 2, 5 & 12 March). Over time the images show a general decrease in the greenness of the crop, although there are still areas of green present. The Novachem Manual states that Diquat will take 4 days to achieve leaf kill, but up to 14 days to achieve stem kill.

Ground truthing was undertaken by Plant & Food Research staff on 7 March 2018. Desiccation was found to have occurred to at least 95% of the potato canopy across the entire paddock, with no clear correlation between the NDVI results from the UAV. There were some potato plants that were identified in the treatments with green stems in the ground truthed plots, but there was no significant difference in the incidence of greening tissue between the “Green” and “Brown” zones. Three plants in one “Desiccated” plot were identified as having purple stems, dead regrowth and also possible CLso, however this incidence was not confirmed by pathology.

Percent greenness at the site decreased from 100% green (before desiccant application) to 0% green at the last flight on 12 March. It is important to note that the UAV imagery allows us to detect greenness in the crop at very low levels. Therefore the NDVI values of the crop are very low, in many case less than 0.2. However, this data does not discern between green foliage that has not been desiccated, and desiccated plants that have begun regreening.

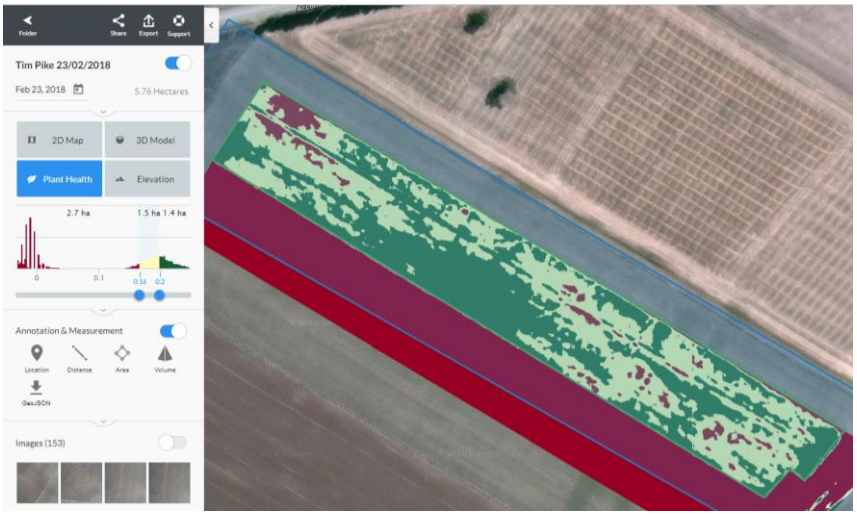

Figure 1 NDVI Image of Site 3 (within black boundary lines) taken 23 February 2018, before desiccant application

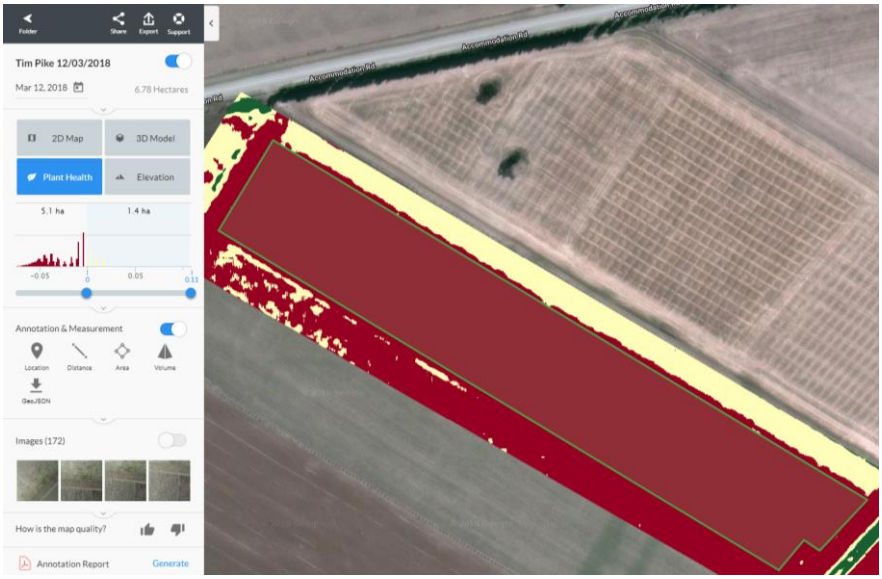

Figure 2 NDVI image of Site 3 (within green boundary lines) on 12 March 2018 showing complete canopy desiccation

PFR assessments taken on 7 March showed that, even though the drone flight NDVI maps showed the desiccation increased over time, ground truthing assessments showed that there was still 1-5% of plants with green tissue visible on the underside of the stems, something the UAV images are unable to detect. Some greening was still visible to the UAV's RGB camera on the 27 February flight.

The use of the UAV images is useful to measure areas of green present in the potato canopy. However, UAV flights were not carried out frequently enough to determine if the greenness measured in the sample crop was green foliage before it changes colour due to desiccation, or if it was desiccate foliage that had begun to regreen. In order to measure this it is necessary to measure the change in canopy greenness from before desiccation.

It is possible to detect areas with different levels of greenness in the crop canopy from UAV data and define areas of the paddock that require a follow-up application of desiccant spray. These areas can then be loaded

into a sprayer controller to enable the sprayer to turn on and off as it travels along the tramlines to only spray the zones identified as having crop regreening.

With rapid development in satellite technologies, and the increasing resolution, it may soon be possible to accurately measure canopy characteristics using satellite data, which may remove the need for UAV flights. Using the most common Sentinel satellite platform, the current resolution of satellite imagery is 9m x 9m, as shown in Figure 3 below. The use of this imagery to identify points in the paddock to undertake ground-truthing may be feasible, but as satellite image resolutions increase, these images may provide enough resolution to accurately target individual plants. Planet Labs latest satellite imagery is available with a pixel size of 72 x 72cm.Internationally, potato producers are using these images to detect early onset of Potato Late Blight.

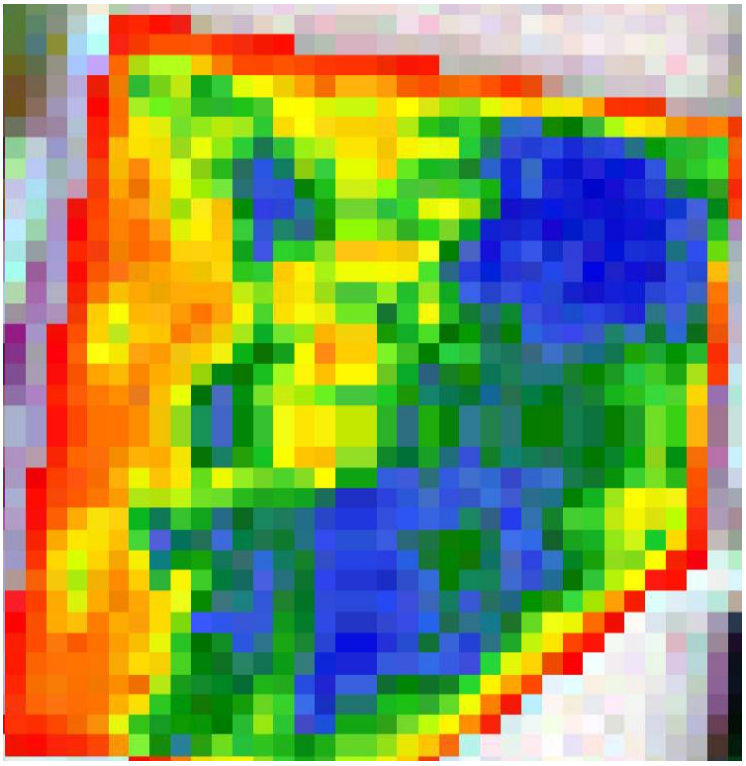

Figure 3 Sentinel Satellite data 23 February 2018

3.2 Desiccation water rates and nozzles

At the initial assessment on 16 February, 3 days post desiccation there was no difference between treatments for the % kill recorded, all treatments recorded 40% kill (60% green leaf retention).

There was a noticeable difference in percent desiccation scores with time over the first four assessments (16 Feb – 2 March), all treatments were above 96.7% for the 5 March assessment (99% mean) with minimal difference between water rates or nozzles.

200L/ha, 300 L/ha and 400L/ha with both nozzles all reached 100% desiccation by 9 March.

Table 1. Mean desiccation scores (percent plant kill) for four water rates (200, 250, 300 and 400L/ha) and two nozzles at each water rate (Potato and Defy) at seven different dates post initial desiccation.

	200L/ha		250L/ha		300L/ha		400L/ha	
Date	Potato	Defy	Potato	Defy	Potato	Defy	Potato	Defy
16-Feb	40	40	40	40	40	40	40	40
23-Feb	63.3	61.7	50.0	48.3	61.7	71.7	56.7	58.3
27-Feb	70.0	75.0	78.3	76.7	75.0	73.3	73.3	73.3
2-Mar	85.0	86.7	86.7	80.0	91.7	93.3	88.3	85.0
5-Mar	100	100	96.7	96.7	100	100	98.3	100
9-Mar	100	100	99.3	99.3	100	100	100	100
13-Mar	100	100	99.3	99.3	100	100	100	100

Figure 4 Photo taken 6 March 2018, ten days after initial desiccant application
Some stems within plots still showing small levels of greenness.

3.3 Ability to detect disease and virus using UAV

The UAV sensing work undertaken this season has proved inconclusive regarding the ability to detect diseased areas of the crop. The NDVI results in the crop are more likely due to underlying agronomic issues with the crop and site interaction, such as difference in soil texture, and therefore crop water stress, as shown in Figure 4 below.

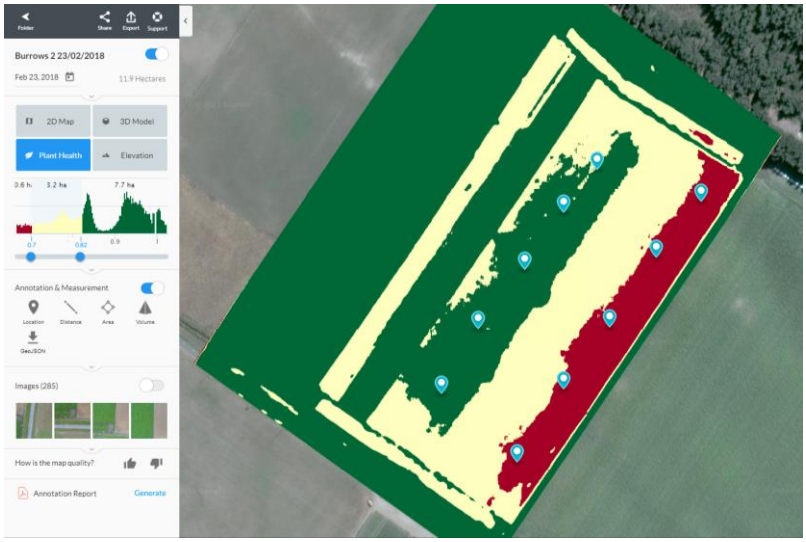

Figure 4 Site 2 UAV image 23 February 2018, showing NDVI and sites for ground-truthing

Images such as those shown in Figure 4 were generated for each UAV flight. While it is possible to zoom into the image at a high resolution, the aim was to identify large scale differences within the crop, and then undertake ground truthing to assess if these zones had different levels of disease. It may be possible to zoom UAV images to a high resolution to try and identify individual plants with disease symptoms, but this was not attempted in this work. By undertaking UAV flights and DroneDeploy it is possible to generate images with pixel resolution of less than 2 x 2cm, as shown in Figure 5 below.

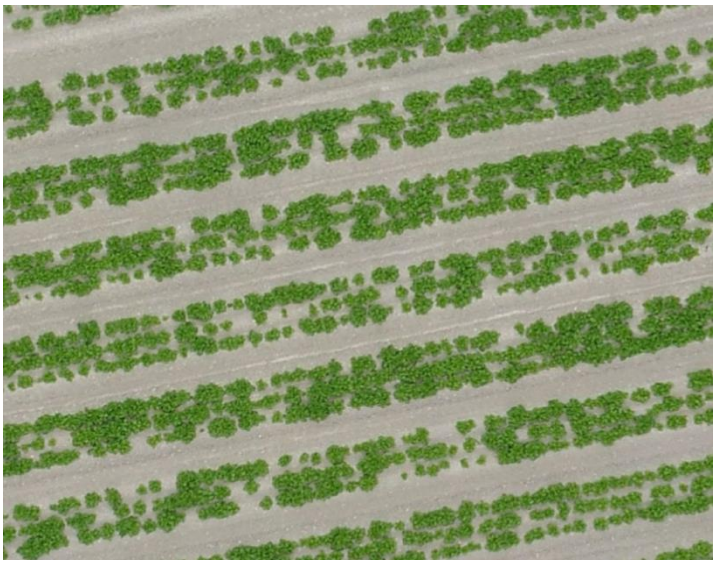

Figure 5 Image from DroneDeploy showing 1.7 x 1.7cm pixel size

Table 2 Groundtruthing Observations Site 1. 7 March 2018.

Sites identified as "Healthy" (shaded green)		
GPS Point	Issue	Notes
038	Plants laid over, slightly yellow	Canopy slightly yellow compared to point 0062. No flowers. Waist high, healthy. Some stems laid over - knee high ~1x5 m. 1-2 small black spots per leaf.
044	Verticillium symptoms	Cupping, yellow, and dieback from ends in ~5 plants in 5x5 m. Knee height. Moderate flowers. Uneven canopy.
046	Verticillium symptoms	Cupping, yellow and dieback at ends ~2-5 metres. Waist high. Minimal flowering. Deep green canopy overall. Less small black spots than other targets.
047	Healthy overall	Waist high. No flowering. Crop doesn't quite meet in some areas. Fairly even canopy. Less small black spots than other targets. Appears healthy overall.
054	Verticillium symptoms	Cupping, yellow, and dieback from ends in plants every ~1m. Sample taken from this point and cut open by pathologist - confirmed verticillium. Spots of dense flowering. Rest of crop waist high and deep green.
Sites identified as "Unhealthy" (shaded orange)		
GPS Point	Issue	Notes
032	Healthy overall. 1 plant CLso symptoms	Canopy tall, dense, and meets. Mostly done flowering. Appears healthy overall. A single plant, where point was taken, showing Clso symptomatic cupping, yellowing, purpling on stem and edge of leaves plus enlarged nodes.
039	Short sparse crop on ridge	Knee high, does not meet. Yellow here compared to lower areas. Point taken in the tramline. No flowers. 1 tall weed every 5 m. 1-2 small black spots per leaf.
040	Short sparse crop on ridge	Some taller plants may have verticillium - more yellow and cupping - dying back at ends. Most crop knee high, does not meet, halfway down from top of ridge. Yellow here compared to lower areas. No flowers. 1 tall weed every 5 m. 1-2 small black spots per leaf. Point taken in the tramline.
056	Healthy overall	Waist high. Dark green. Minimal flowering. Minimal black spots. 1 yellow planting a 10 m radius. Some variation in height - Some lines of plants laid over.
057	Healthy overall	Waist high. Dark green. Minimal flowering. Minimal black spots. 1 yellow planting a 10 m radius. Some variation in height - Some lines of plants laid over. Canopy meets.

Tables 2 and 3 show the results from the ground truthing of the points identified from the UAV image data at Site 1 on 7 March; and Site 2 on 8 March. It can be seen that there is no relationship between the points identified in areas of high NDVI, shaded green, and low NDVI, shaded orange, and any incidence of disease

Table 3 Groundtruthing Observations Site 2 March 8 2018.

Sites identified as "Healthy" (shaded green)		
GPS Point	Issue	Notes
059	Healthy overall	Some gaps where canopy should meet - several metre portions of rows laid over. Knee high. Deep green. Full inflorescences.
060	Healthy overall	Some gaps where canopy should meet - several metre portions of rows laid over. Knee high. Deep green. Full inflorescences.
061	Healthy overall	Some gaps where canopy should meet - several metre portions of rows laid over. Knee high. Deep green. Full inflorescences. A few plants showing minor down/up curling on partially malformed leaves but no colour change - minor.
062	Healthy overall	Just below ridge ~30 m from top. Some gaps where canopy should meet - several metre portions of rows laid over. Knee high. Deep green. Full inflorescences. A few plants showing minor downward curling on partially malformed leaves but no colour change - minor.
063	Healthy overall	Almost waist high. Deep green. Full inflorescences. ~15 m past ridge crest - area appears to be a knob, slopes to corner fence lines. Similar to other points, some gaps where canopy should meet, plants laid over.
Sites identified as "Unhealthy" (shaded orange)		
GPS Point	Issue	Notes
066	Healthy overall	Knee high. ~30 m down from ridgeline. Full inflorescences. Canopy meets. Small gaps <1 m - plants laid over.
067	Healthy overall	Waist high. Full inflorescences - appear more frequent in this section. Few gaps. Canopy meets. ~5 plants in 5x5 m area with minor downward curling on partially malformed leaves.
068	Healthy overall	Waist high. Full inflorescences - appear more frequent in this section. Few gaps. Canopy meets. ~5 plants in 5x5 m area with minor downward curling on partially malformed leaves.
069	Healthy overall	Waist high. Full inflorescences - appear more frequent in this section. Few gaps. Canopy meets. ~5 plants in 5x5 m area with minor downward curling on partially malformed leaves. 1 plant with stem rot. On slight rise this section - slopes to main road.
070	Healthy overall; 1 plant with blackleg	Waist high. Full inflorescences - appear more frequent in this section. Few gaps. Canopy meets. ~5 plants in 5x5 m area with minor downward curling on partially malformed leaves. 1 plant with blackleg - confirmed by pathologist.

4. Discussion

The water rates and nozzle trial was conclusive showing limited difference between treatments thus 200L/ha is a sufficient rate for haulm kill. There may be variety differences but a key outcome would be to develop an industry standard for desiccation, thus a second year looking at non-chemical desiccation options in conjunction with chemical desiccation could be of value. The ability to use a chemical desiccant such as Reglone® may be limited in future so alternative practices need to be developed.

The trial work this season showed that there are spatial patterns in the level of canopy greenness and this could be an option. However there was no clear correlation between the NDVI values generated from the UAV images to the level of greenness present in the field, in order to be of value careful consideration needs to be given to calibrating the UAV generated NDVI value to actual canopy greenness. Next seasons' work should move towards correlating NDVI maps with sprayers and only applying herbicide to areas identified as still green. The ability to detect virus and disease using data generated from UAV flights was challenging.

5. Recommendations

In order to fully investigate regreening in potatoes future research should carry out more regular UAV flights and ground-truthing beginning before initial desiccant application to attempt to identify early incidence of disease in the crop, and correlate with UAV imagery.

To investigate the ability of UAV's early incidence of disease in the crop, it is possible that the use of UAVs with different sensors will increase the chance of identifying disease incidence in the crop to identify regreening in potatoes. Future research should consider establishing a trial paddock with plots of different potato cultivars and seed lines with different susceptibility to disease and carry out more regular UAV flights and ground-truthing.

6. Acknowledgements

We wish to thank the growers who provided paddocks and assisted with desiccation, the team at Plant &Food Research for ground truthing and FAR staff for in-season assessments. Thanks also go to AgriOptics for conducting the drone flights. The project receives funding from MPI Sustainable Farming Fund and Potatoes New Zealand.

7. Appendices

7.1 Appendix 1: Methodology for Determining and loading Sampling Points from UAV Images

1. Images from UAV flight loaded into Drone Deploy

2. Zoomed image below shows possible resolution (1.7 x 1.7cm pixel size)

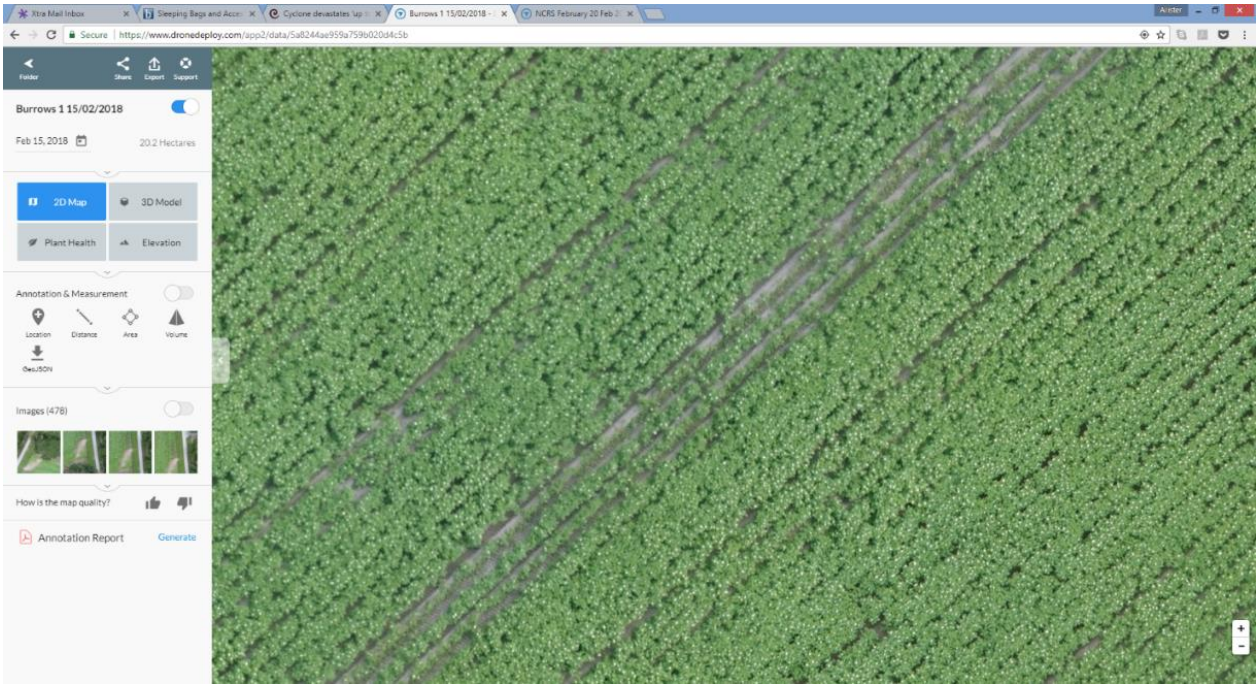

3. Use of “Plant Health” functions to identify three zones – high, medium and low NDVI

4. Manually place points on areas of interest:

5. Image below shows size of zone of interest – 37m wide green strip

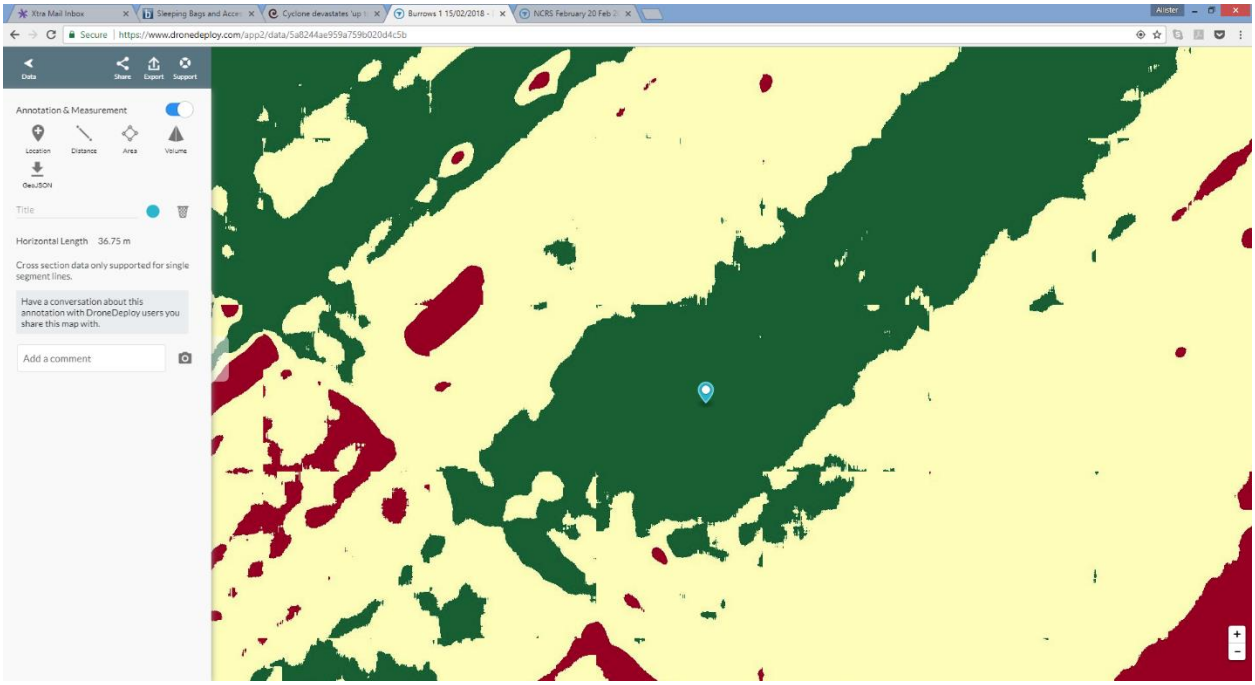

6. Points overlaying aerial RGB image

7. Export location coordinates as a JSON file
8. Convert JSON file to GPX file using https://mygeodata.cloud/converter/
9. Import GPX file into Garmin Basecamp
10. Save GPS coordinates to handheld GPS

7.2 Appendix 2: Images produced over time from Accommodation Road site - Using Precision Agriculture tools to detect re greening following desiccation

23 February 2018 – Pre desiccation RGB image (1.7 x 1.7cm pixel size)

27 February 2018 – desiccation occurring

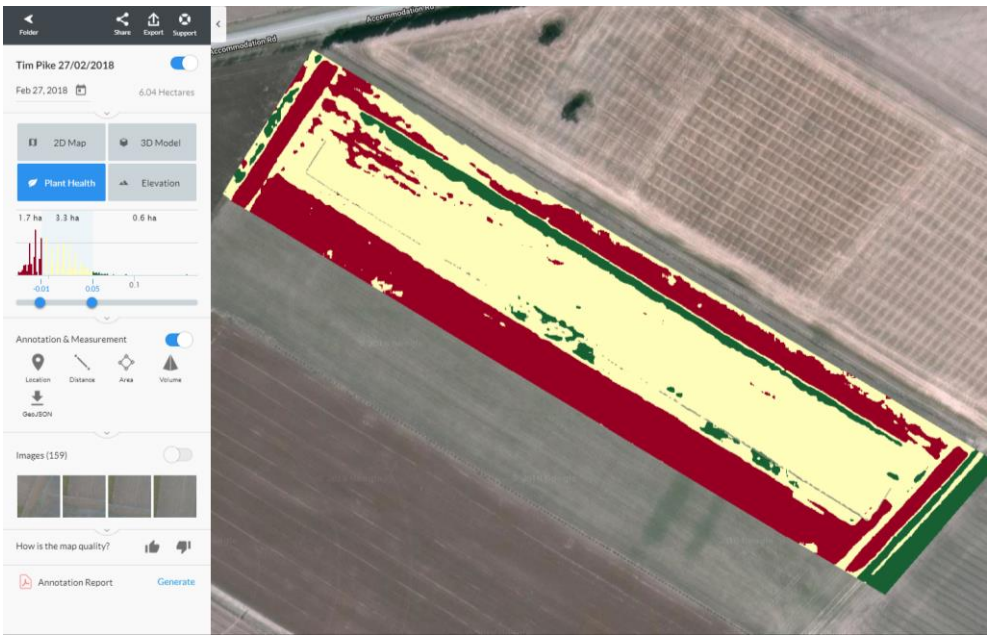

12 March 2018

7.3 Appendix 3: Site 1 - Ability to detect disease and virus using UAV

Site 1 - 1 March 2018 RGB image

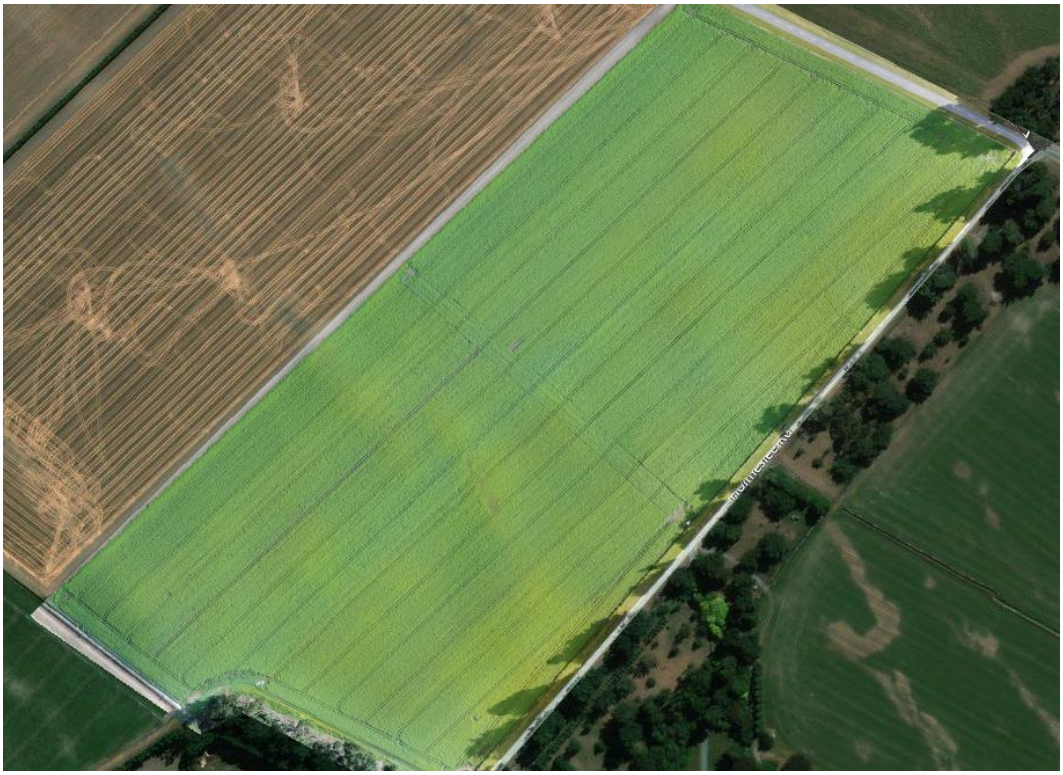

Site 1 - 1 March 2018 NDVI image

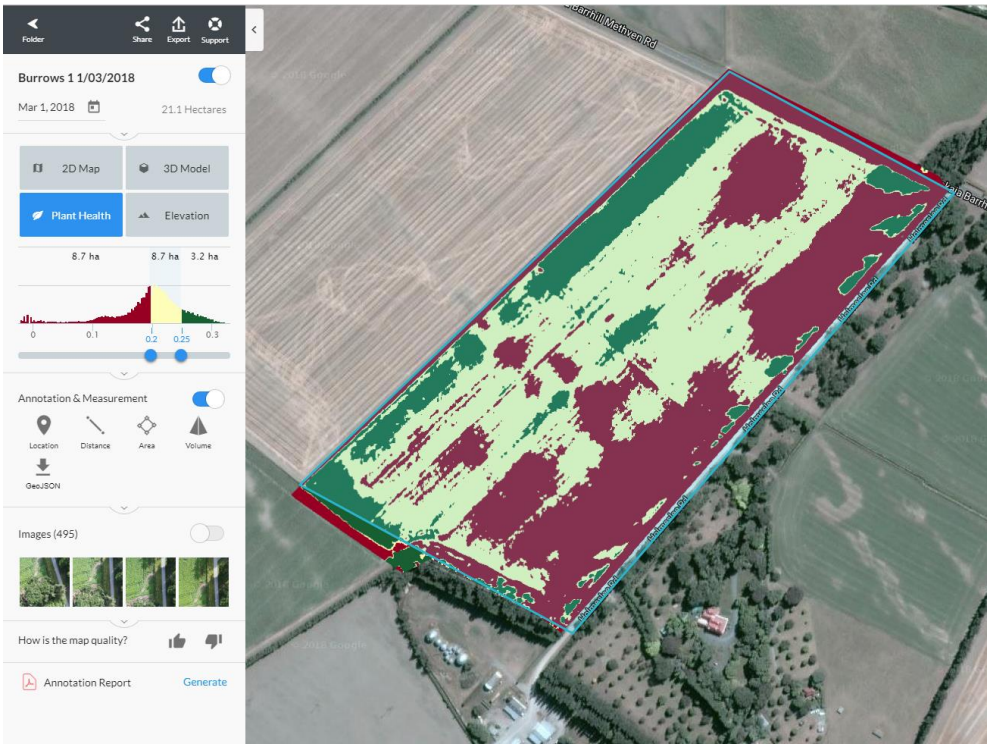

Manaaki Whenua
Landcare Research

Hyperspectral Signature of cLSO Infection of Seed Potatoes - a Shadehouse Experiment

Prepared for: Potatoes NZ

September 2019

Hyperspectral Signature of cLSO Infection of Seed Potatoes - a Shadehouse Experiment

Contract Report: LC[Editor will add]

Andrew M.S. McMillan

Manaaki Whenua – Landcare Research

Reviewed by:	*Approved for release by:*
Pierre Roudier Research Scientist Manaaki Whenua – Landcare Research	…

Contents

Summary

Project and Client

- Project: Improving the quality of seed potatoes using precision agriculture – A Sustainable Farming Fund (SFF) Project
- Client: Potatoes NZ – Lead contractor for the SSF Project.

Objectives

- Investigate whether the CLso symptoms can be detected using hyperspectral imaging of the foliage of CLso-infected and uninfected potato plants

Methods

- Experiment 1. Infected (n=10) and healthy (n=10) Russel Burbank tubers were planted and grown in pots in a shadehouse at Lincoln on 23 October 2018.
    - Close-range (92 cm) hyperspectral imagery was collected for each plant on five occasions at 31, 35, 38, 48 and 52 days following planting.
- Experiment 2. Healthy tubers of Russel Burbank (n=20) and Innovator (n=20) were grown in pots. They were planted on 21 October 2019. On 23 January 2019 half of the plants in each cultivar group were infected with CLso via the Potato Psyllid vector.
    - Close-range hyperspectral imagery was collected for each plant on 10 occasions at beginning one day before infection and ending 54 days after infection (95 to 150 days following planting).
- Raw hyperspectral imagery (HSI) was converted to reflectance using Headwall Photonic's SpectralView software, and customised Python and R scripts were used to assess differences between infected and uninfected plants.

Results

- Experiment 1: Detecting CLso in plants from infected tubers
    - Variability in the spectra among replicate plants was of similar magnitude to differences between healthy and infected plants. This prevented CLso-detection that is purely based on the shape of the spectra.
    - However, we found significant differences between healthy and infected plants in the amount of leaf area with NDVI values between 0.8 to 0.9 at 30 days following planting.
- Experiment 2: Detecting CLso in plants infected with CLso via transmission from potato psyllids.
    - Spectral analysis, rather than the NDVI-class Green Area approach used in Experiment 1, was the preferred method of detecting CLso transmitted by psyllids.

- There were marked differences in the spectral reflectance between infected and non-infected plants, and between the two cultivars tested. Infected plants tended to be higher in the visible region from 570-650 nm and in the near-infrared region between 730 and 930 nm These differences provided the basis for early detection of CLso but further work is required to determine how this benchtop experiment could be translated to operational field conditions.

Conclusions

- Early stage tuber-transmitted CLso-infection was detected by measuring the leaf area within an NDVI class of 0.8 – 0.9.
- A large proportion of early state psyllid-transmitted CLso-infected plants could be detected within two days by searching for anomalously high reflectance in the 570-650 nm in Innovator cultivar and at nine days in the Russet-Burbank cultivar.
- Since the differences between infected and healthy plants persist across a wide range of wavelengths, there is a reasonable prospect that a moderately-priced multispectral sensor (rather than an expensive hyperspectral sensor) could be flown by a drone over a potato crop and used to detect individual plants with the disease at an early stage.

Recommendations

- The findings from this shadehouse study indicated that there is a basis for spectral sensing of CLso-infected plants in a commercial potato crop setting.
- The next step is to determine whether individual CLso infected potatoes can be detected using the spectral approaches outlined multispectral cameras mounted on drones.
- We provide an outline for testing the results of this shadehouse experiment in the field with a view to developing an operational algorithm.

1 Introduction

The bacteria *Candidatus* Liberibacter solanacearum (CLso) is associated with the zebra chip disease of potatoes (Pitman et al., 2011), an economically important disease that can cause yield losses of up to 60% (Pitman et al., 2011. CLso can be transmitted to a potato crop by the potato psyllid, *Bactericera cockerelli*. Alternatively, infected mother tubers can act as a source of the bacteria.

Foliar symptoms of plants affected by zebra chip vary widely, but include an upward rolling of the basal portion of young leaves, chlorosis, purple top, shortened internodes, small leaves, enlargement of the stems, swollen auxiliary buds, aerial tubers and early plant senescence (Pitman et al., 2011).

Plants with CLso transmitted via the mother tuber exhibit the following symptoms: (a) germination failure; (b) successful germination but a spindly growth habit; (c) germinate and grow a non-diseased plant, or d. germinate and grow a diseased plant (and subsequently infected daughter tubers) (Pitman et al., 2011).

The purpose of this project was to investigate whether hyperspectral imaging could assist in early detection of this disease in potato plants. Our objective was to determine whether there is a hyperspectral signature for (a) plants grown from CLso-infected tubers; and (b) plants infected with CLso via transmission by the potato psyllid.

2 Background

Hyperspectral imaging is a technique of spectral imaging that can be compared to standard RGB photography. A standard RGB camera captures an image where each pixel contains information on just three spectral bands — we think of them as colours: red, green and blue. By contrast, each pixel of a hyperspectral image image contains information on hundreds of spectral bands — they may be thought of as finely resolved colours, but it is more correct to think of them as different wavelength bands. They often extend beyond the visible region of the electromagnetic spectrum and into the near-infrared and shortwave infrared.

Generically, plant stress causes changes to the spectral reflectance of leaves. Factors such as nitrogen deficiency can reduce the abundance of chlorophyll and other pigments, leading to greater reflectivity in the visible region (Carter, 1993). Hyperspectral sensing has been used extensively in the detection of plant diseases (Lowe et al., 2017; Mishra et al., 2017) and recently for the detection of Potato Virus Y in seed potatoes (Polder et al., 2019) using deep learning algorithms. However, a literature search revealed no publications on the use of hyperspectral imaging for the detection of foliar symptoms of CLso in potatoes, although benchtop hyperspectral imaging was used to detect the presence of Zebra Chip symptoms in potato tubers (Zhao et al., 2018).

3 Objectives

1. Set up and test an imaging system to capture hyperspectral imagery of potted potato plants in a shade house;

2. Use the system to monitor the spectral reflectance of potatoes infected with CLso via infected mother tubers (Experiment 1) and potatoes infected with CLso via the potato psyllid (Experiment 2);

3. Process and analyse the hyperspectral imagery with a view to developing an operational methodology for an 'early warning' system to be used in the field.

4 Methods

4.1 Growth of experimental plants and infection with CLso.

A detailed description of the preparation of the test plants and infection is provided in Vereijssen et al. (2019). However, a brief description of the experimental set-up is provided below.

4.1.1 Experiment 1. Investigation of the hyperspectral signature of potatoes infected with CLso via the infected mother tubers

Ten tubers of CLso-infected potato cultivar Russet-Burbank were germinated and grown in 4 L plastic pots together with ten identical but uninfected tubers as control specimens. They were planted on 23 October 2018 and placed in the shadehouse for hyperspectral imaging on 21 November 2018.

4.1.2 Experiment 2. Investigation of the hyperspectral signature of potatoes infected with CLso via the potato psyllid

Twenty tubers each of potato cultivars Russet-Burbank and Innovator were tested for presence of CLso via qPCR (Beard & Scott, 2013). All tested negative for CLso (data not presented).

On 19 October 2018, each tuber was planted 10 cm deep in a 4 L plastic pot in standard non-sterile potting mix filled 4 cm from the top at Plant & Food Research, Lincoln. Pots were moved to a shade house, where a tray was placed underneath each pot to act as a water reservoir and to assist even watering between pots. Tubers were watered thoroughly after planting and then once or twice weekly depending on their requirements.

On 23 January, nine weeks after planting, one leaf on 10 plants of each cultivar were exposed to CLso-positive *B. cockerelli*. The adding of the psyllids was delayed by 10-14 days because of non-availability of the hyperspectral camera. A mesh organza bag (Manufacturer MegaView Science) was placed over a leaf of a plant, and vial containing 5 psyllids was carefully placed in the bag. The psyllids were on the plant for 2 weeks, and

during this time the potato plants were scanned with a hyperspectral camera. The leaf with the organza bag was removed from the plant on 5 February 2019. Then, a tuber sample of each plant was tested for presence of CLso using qPCR according to Beard and Scott (2013). All plants within the control treatment tested negative for CLso, and all but two of the plants in the infected treatment tested positive. The two plants where infection was attempted but failed were replicates 'D3' and 'D5' from the ten Innovator cultivar replicates and the spectral information was removed from subsequent statistical analysis.

4.2 Hyperspectral Imaging

We used a Nano Hyperspec hyperspectral camera (Headwall Photonics, MA, USA). This is a line scanning camera with a 'push-broom' action, meaning that a single image consists of a spatial line of pixels in the x direction, but only 1 pixel in the y direction. However, each of the pixels within that single line contains data points for each spectral band. For this camera, there are 640 pixels in the x-direction, 1 pixel in the y-direction and 274 different spectral bands, ranging from 398 nm to 1004 nm. This spectral range encompasses the visible region (400 nm – 750 nm) and the near-infrared region (750 nm – 1000 nm). Accordingly, such a hyperspectral camera is known as a VIS-NIR camera.

To collect images of the potted potato plants, we designed and fabricated a gantry camera slider (Figure 1), that allowed the camera to be moved above the plants in the y-direction at a constant rate. The velocity of this motion was set according to the incident radiation and the corresponding exposure requirements of the camera. Eight hundred separate images (or lines) of data were collected over the travel distance of the camera slider (which moves in the y direction) resulting in a hyperspectral 'cube' of data with the following dimensions: 640 pixels width × 800 pixels height × 274 spectral bands.

In Experiment 1 (the infected tuber experiment), each plant was imaged a total of five times at 31, 35, 38, 48 and 52 days after planting. In Experiment 2 (the psyllid-infection experiment) each plant was imaged a total of 10 times between 95 and 150 days following planting (and ranged between one day before and 54 days after infection with CLso via the psyllid vector). The experimental timeline is provided in Table 1.

Figure 1 A Headwall Photonics Nano hyperspectral camera mounted on automated gantry system. The camera slides along the rail at a velocity proportional to the amount of incident light. Potato plants were scanned in pairs. A single scan of the plants collected a hyperspectral 'cube' consisting of 800 lines of 640 pixels × 274 spectral bands. The card lying between the plants acts as a reference to convert radiance into reflectance.

Table 1 Experimental details and timeline

Experiment 1 - Comparing plants infected with CLso via CLso-infected mother tubers

Varieties tested: Russet-Burbank

Number of replicates:	10 in each of the infected and control treatments
Day of planting	23/10/2018

Hyperspectral Image Acquisition Dates

Sampling #	Date	Days Since Planting
1	23/11/2018	31
2	27/11/2018	35
3	30/11/2018	38
4	10/12/2018	48
5	14/12/2018	52

Experiment 2 - Comparing plants infected with CLso via the potato psyllid

Varieties tested: Russet-Burbank, Innovator

Number of replicates	10 in each of the infected and control treatments for each cultivar (40 Plants total)
Day of planting	19/10/2018
Day of CLso infection via psyllid	23/01/2019

Hyperspectral Image Acquisition Dates

Sampling #	Date	Days Since Planting	Days Since Infection
1	22/01/2019	95	-1
2	25/01/2019	98	2
3	1/02/2019	105	9
4	7/02/2019	111	15
5	12/02/2019	116	20
6	20/02/2019	124	28
7	27/02/2019	131	35
8	4/03/2019	136	40
9	11/03/2019	143	47
10	18/03/2019	150	54

4.3 Image Processing

4.3.1 Conversion of raw data to radiance

The hyperspectral camera collects raw data as uncalibrated digital numbers. These were converted to a physical radiance value with units of mW $[cm^2.sr.\mu m]^{-1}$. This was done using the camera's post-processing software SpectralView version 5.5.1 (Headwall Photonics, MA, USA). SpectralView uses a camera-specific factory calibration for each pixel and the manufacturer's recommended dark calibration, which was conducted at each sampling occasion in the shadehouse. Using this software, we created a radiance image for each raw image. Each radiance image had identical dimensions to its corresponding raw image (640 pixels width × 800 pixels height × 274 spectral bands).

4.3.2 Conversion of radiance data to reflectance

Each image contained two potato plants in pots together with a calibration card in the middle. The calibration card had three panels with standardised reflectance of 1%, 18% and 99% for the black, grey and white panels, respectively (Figure 2). A Python software program was developed to iterate through the radiance images and allowed the user to draw a four-sided polygon with the mouse over the area of the image that corresponded to the white, grey and black panels. From the average reflectance of the black and grey panels, a two-point linear transform function was calculated, and then used to convert each radiance image to a reflectance image (where each pixel is a reflected radiance as a proportion of incident (incoming) radiance at each spectral band.

4.3.3 Detection of Plant Area

To distinguish living leaf tissue area from non-plant material or dead tissue, we used the spectral vegetation index Normalised Difference Vegetation Index (NDVI) (Tucker, 1979). The formula for NDVI is:

NDVI = (NIR – Red) / (NIR + Red)

We defined red as the average reflectance over the spectral range from 630 to 690 nm and NIR as the average reflectance over the spectral range from 770 nm to 900 nm.

NDVI values were calculated for each image and used as a masking variable to detect living plant area. For experiment 1, a NDVI threshold of 0.5 was used as a criterion to detect plant tissue. Lower NDVI threshold values led to confusion between the plant and non-plant areas of the image.

4.3.4 Processing of hyperspectral reflectance data for each plant

For each pixel of plant material in each image, the following metrics were calculated: (a) reflectance within each spectral band; (b) average reflectance across 20 nm spectral ranges; (c) a variety of spectral vegetation indices in addition to NDVI. We then collected statistics — mean, median, standard deviation, minimum, maximum and 5^{th}, 10^{th}, 25^{th} percentiles — on each of these metrics across each plant. Only statistics for NDVI, the

single band reflectance and the 20 nm band averages were found to be useful for CLso detection and other metrics are not discussed further.

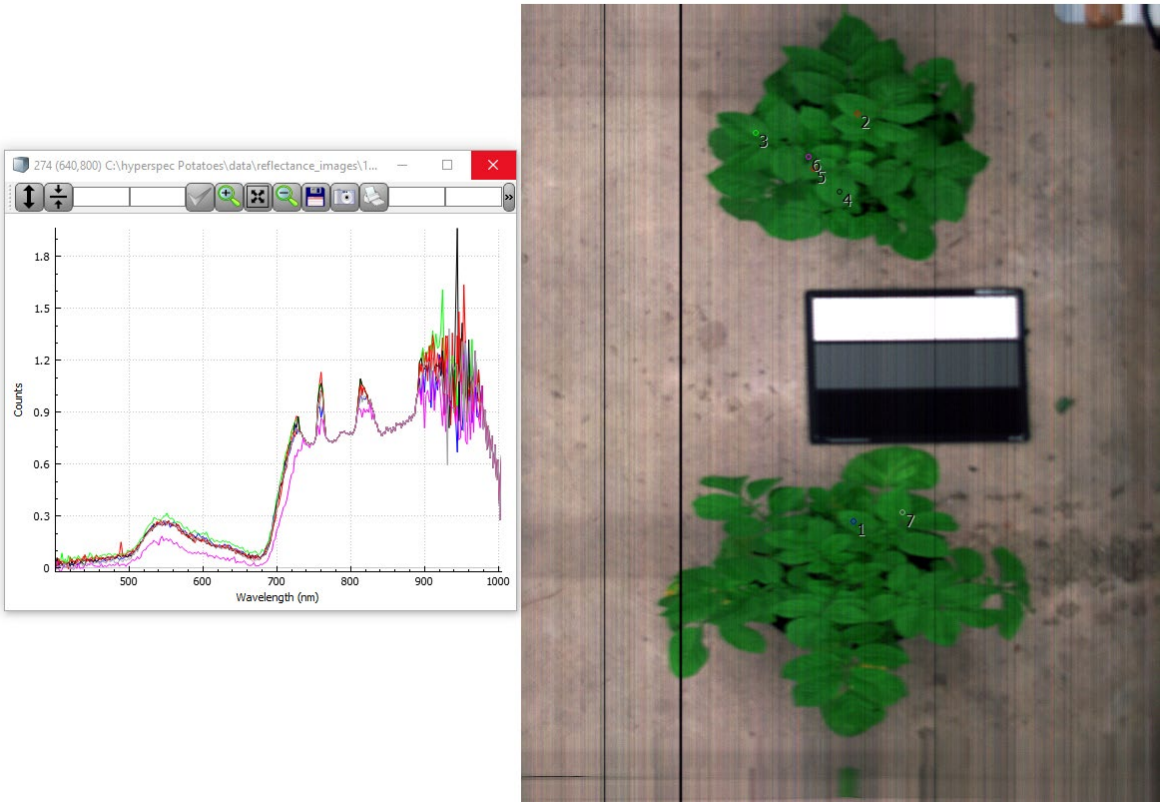

Figure 2 The right panel shows an example hyperspectral reflectance image of an infected plant (top) and a healthy plant (bottom). The radiance is converted to reflectance by imposing a linear transform over the entire image so that reference card in the centre gives reflectance value of 18% (grey panel) and 1% (black panel). The left panel shows the reflectance spectra for selected points on the image.

5 Results

5.1 Plant Growth

The results of the plant growth were reported in Vereijssen et al. (2019). Briefly, in Experiment 1 plants remained green and healthy over the duration of the experiment. However, plants emerging from infected tubers tended to be smaller but greener. Plants emerging from the uninfected tubers tended to be larger but had visual signs of senescence.

In Experiment 2, heat conditions in the shade house caused plant stress and resulted in senescence across all plants, which complicated the hyperspectral analysis.

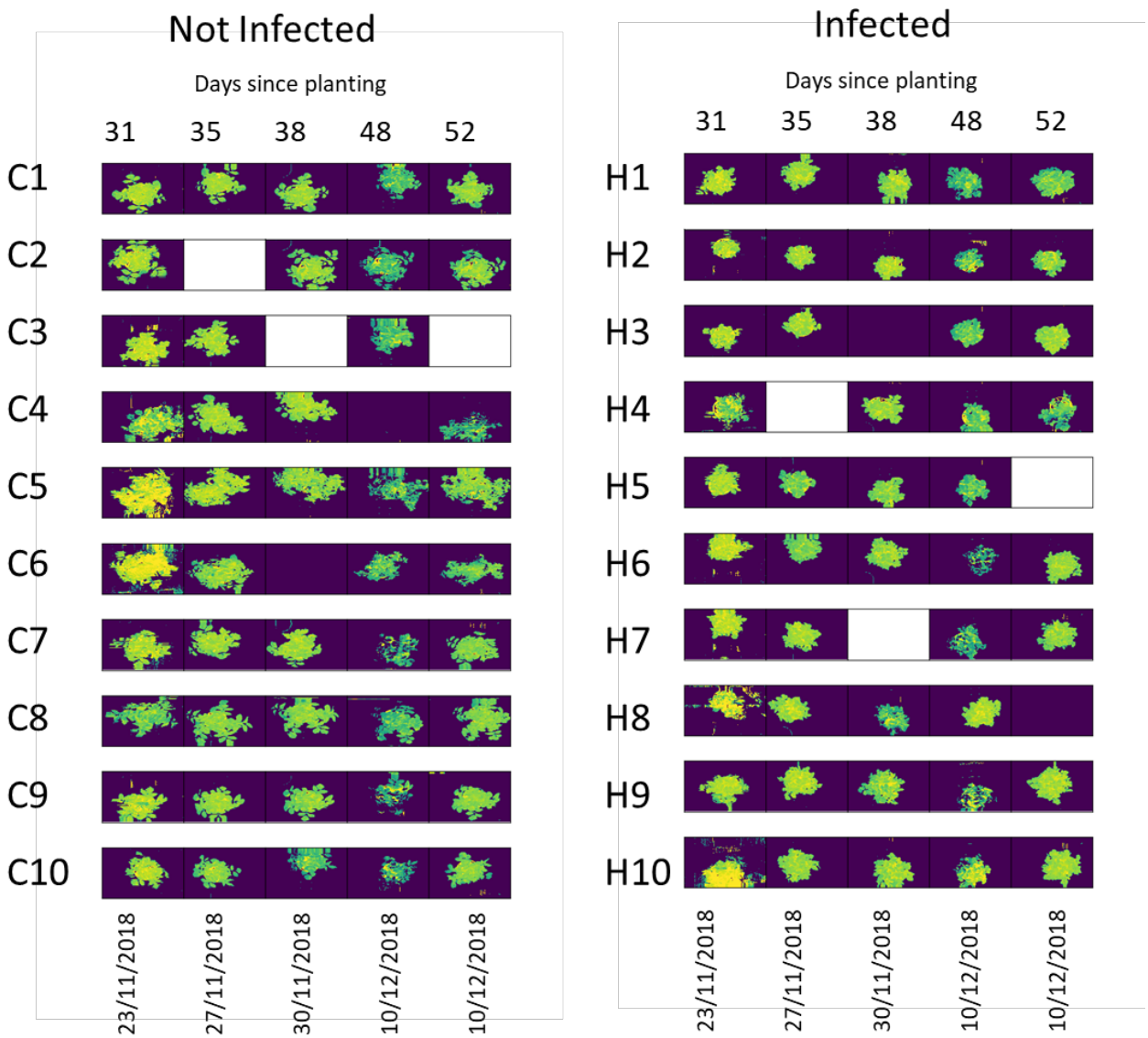

Figure 3 NDVI images of 10 infected and 10 non-infected plants from Experiment 1. H1-C10 refer to individual plant idenitification numbers.

5.2 Experiment 1 – Comparing Clso-Infected and Healthy Tubers

5.2.1 Image collection

A total of 258 hyperspectral images were collected: 50 were collected during Experiment 1 on 5 separate sampling occasions; 208 were collected during Experiment 2 on 10 separate sampling occasions. The NDVI-masked images for Experiment 1 are shown in Figure 3 and for Experiment 2 in Figure 10 through Figure 13 in the Appendix.

Some problems were encountered with heat in the shade house deforming the plastic components of the gantry leading to uneven motion of the camera and low quality imagery. This led to the rejection of five images in Experiment 1.

5.2.2 Green area of individual plants

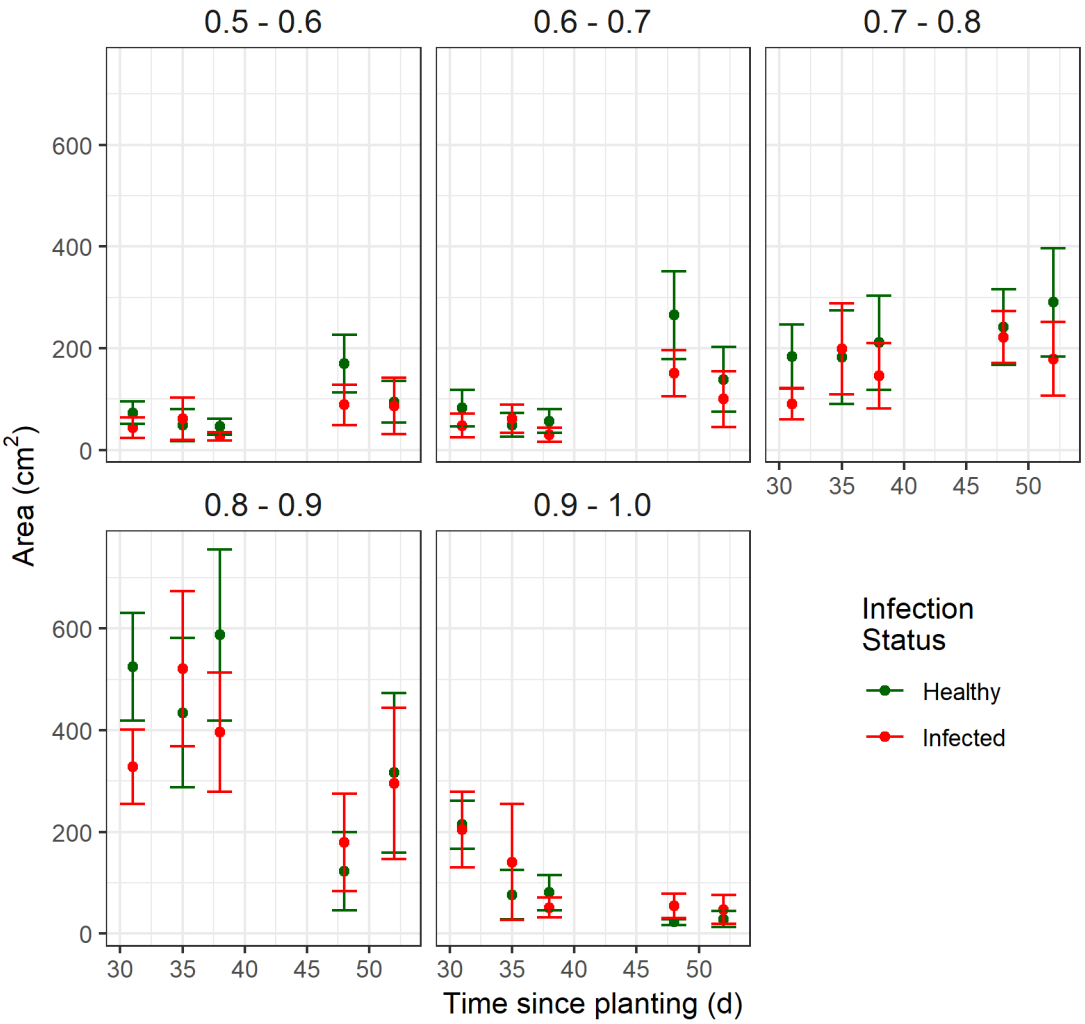

Figure 4 Leaf area in five different NDVI classes in Experiment 1 – comparison of infected and healthy tubers. Panel labels indicate the range of NDVI. Error bars denote 95% confidence intervals

Overall the variation in total green area was not significantly different dur to a large amount of variability among replicates (data not shown). This may be explained by the

opposing effects of smaller plant size in the infected plants and a greater level of senescence in the uninfected plants.

However, when the data was separated into different classes of greenness (measured here by NDVI calculated on a per-pixel basis), we could distinguish between healthy and infected tubers at day 31 within the NDVI class 0.8 to 0.9 (Figure 4).

5.2.3 Spectra at different sampling dates during Experiment 1

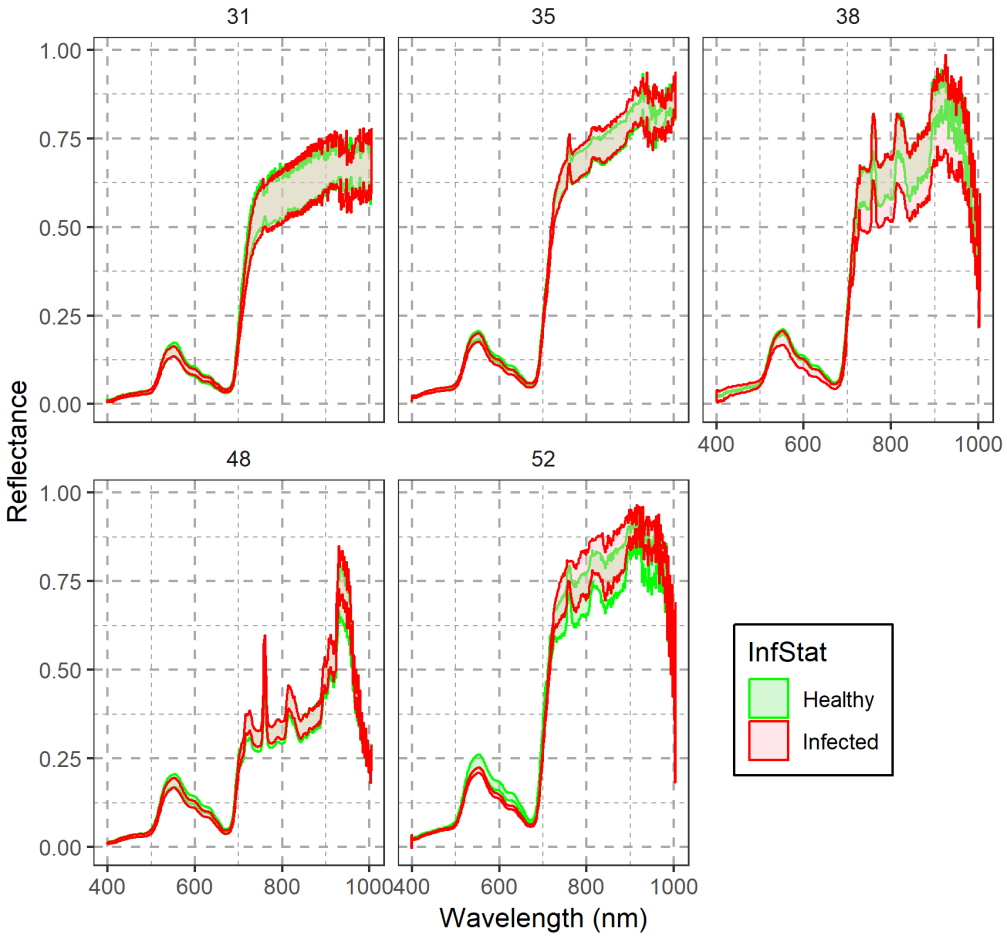

Figure 5. 90% Confidence intervals of spectral reflectance for potato plants with healthy and infected tubers at five time points. Numbers at top of panel indicate days since planting.

Overall, the spectra showed characteristic patterns consistent with the literature (for example, Carter and Knapp (2001)) (Figure 5). Reflectance is generally lower and less variable in the visible region (400-740 nm) with an obvious local peak in the wavelengths corresponding to green reflectance (around 550 nm). The steep increase in reflectance from ~680 nm to ~750 is known as the "red edge" and its position and shape contain information regarding chlorophyll content, biomass and hydric status (Filella and Penuelas, 1994). Reflectance at higher wavelengths (750 to 1000 nm, known as the "Near Infrared Region or NIR"). Reflectance in this region was more variable among replicates, and increased less sharply and less smoothly with increasing wavelength then reflectance in

the "red edge" region. The signal-to-noise ratio for the camera's sensor decreases markedly above 900 nm and the usefulness of reflectance values above 900 nm is limited.

The spectra differed markedly over the course of Experiment 1, but were remarkably similar between treatments. This suggests that inspection of the spectra alone would not provide a satisfactory basis for detection of plants emerging from infected tuber. Our analysis of spectral vegetation indices, in addition to NDVI, did not reveal obvious differences between infected and uninfected plants.

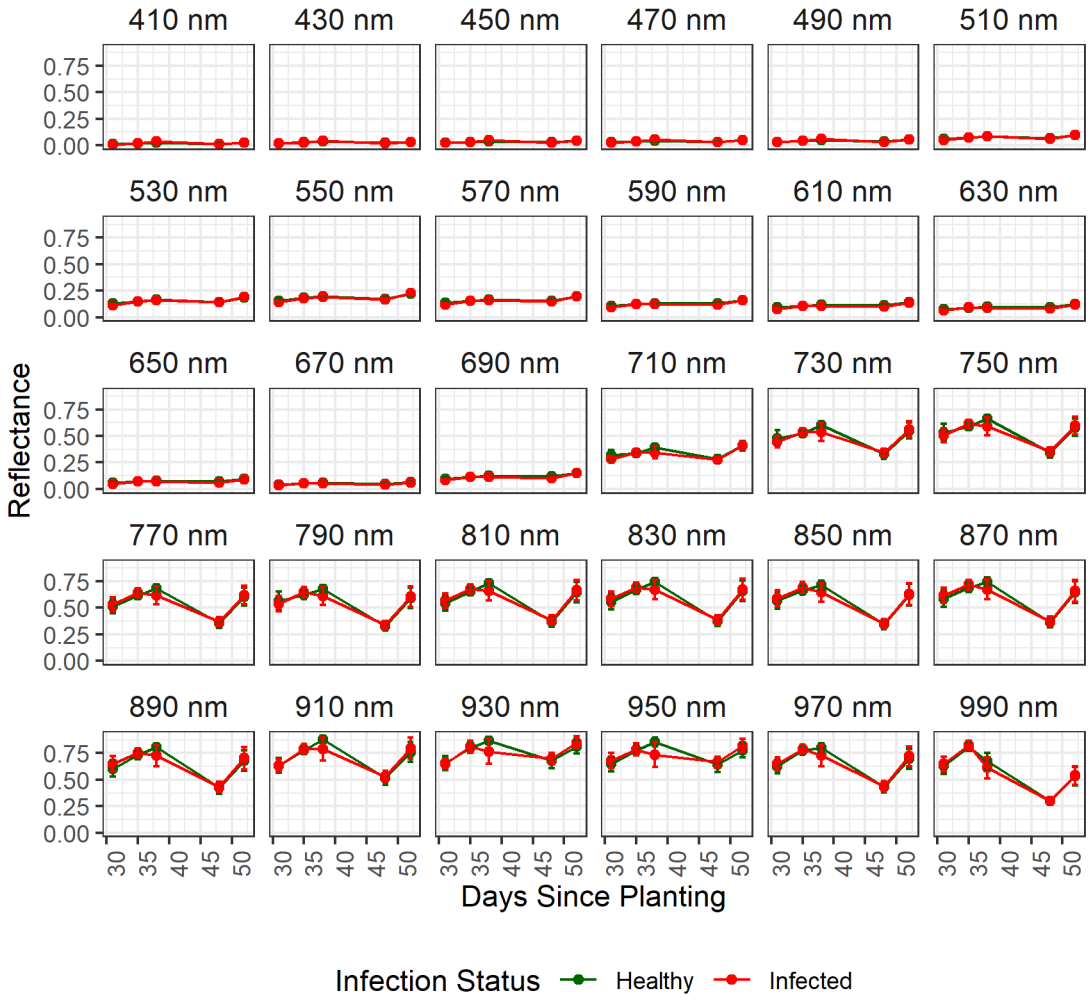

Figure 6. Mean reflectance of plants in Experiment 1 within different spectral bands of 20 nm width centred on the wavelength in panel label. Error bars represent 95% confidence intervals.

The similarity between healthy and infected plants is underscored in Figure 6 where significant differences at any wavelength region were not apparent.

We undertook three other lines of analysis to form a detection algorithm for infected tubers. First, we calculated a large number of spectral vegetation indices (Table 1). Second, we tried differentiation of the red edge – an approach suggested by Filella and Penuelas

(1994). Finally, we tried a simple machine-learning approach known as Support Vector Machines (SVM). None of these techniques were successful in reliably distinguishing between infected and non-infected plants at an early stage.

In summary, we did not find a distinct hyperspectral signature characteristic of plants grown from CLso-infected tubers. However, the camera was useful in allowing us to calculate NDVI – a more reliable measurement of greenness than RGB imagery and comparing the plant area within an NDVI range of 0.8-0.9.

5.3 Experiment 2 — Infected Tubers

5.3.1 Amount of Green Area

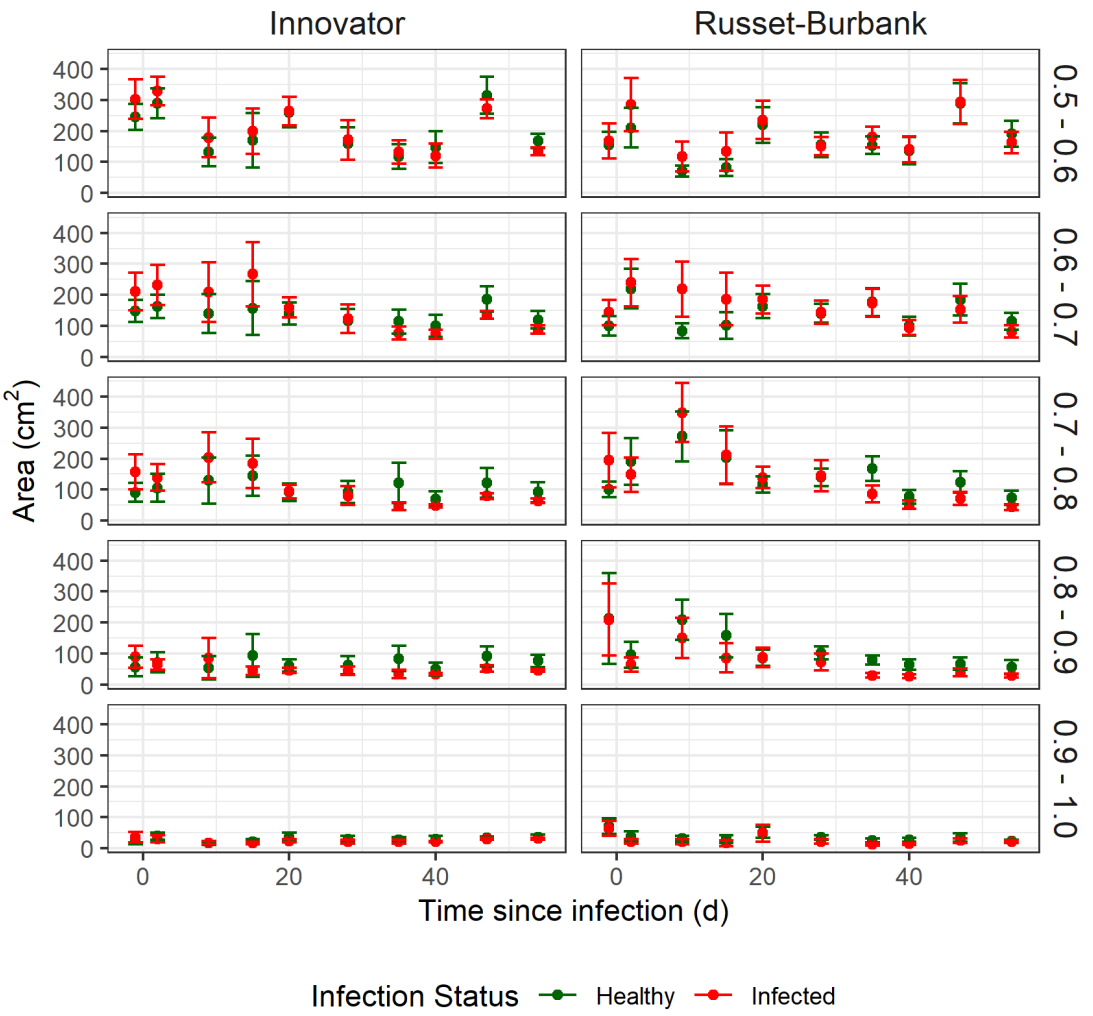

Figure 7 Green leaf area Median (± 90% confidence interval) in five different NDVI classes and two different cultivars of potato in Experiment 2 (Psyllid-infected Trial). Panel labels on the right-hand side indicate the lower and upper bounds of the NDVI class.

The quantification of the green area within different NDVI classes was not significantly different between infected and healthy plants, and accordingly would not form a reliable basis for the detection of plants infected with CLso via the potato psyllid vector. Large overlapping confidence intervals during the early stages of infection would preclude us using a simple green-area as an early warning basis for the disease (Figure 7).

At later stages (>30 days) in the experiment, the presence of non-overlapping error bars indicated that separation based on the amount green area within the 0.7-0.8 and 0.8-0.9 NDVI ranges. However, since the goal of this research was to seek an 'early warning' detection algorithm, we did not further pursue this possibility.

5.3.2 Spectral differences between infected and uninfected plants in first 20 days since infection

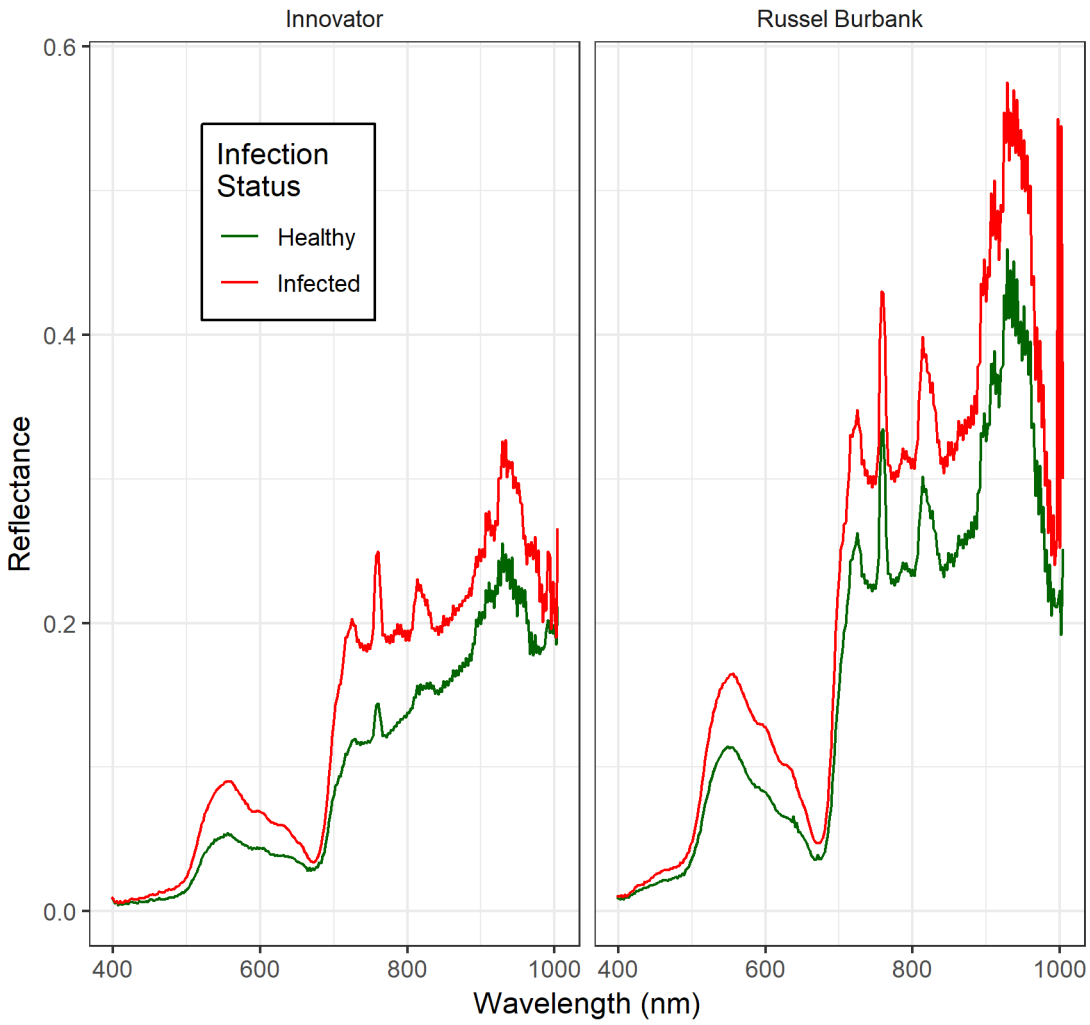

Figure 8 Median Spectra over all wavelengths for Experiment 2 from before infection until 20 days after infection (Comparing Psyllid-infected plants).

The median spectra over the first 20 days and over all replicates in Experiment 2 indicated that infected plants generally had greater levels of reflectance across the entire spectral range. The slope of the "red-edge" region was greater in the infected potatoes than the healthy plants. Substantial differences between the two cultivars also occurred. The Russet-Burbank cultivar was almost twice as reflective as the Innovator cultivar. Spectral features in the NIR were more pronounced in the Russet-Burbank plants.

5.3.3 Range of spectra among replicates during first 20 days since infection

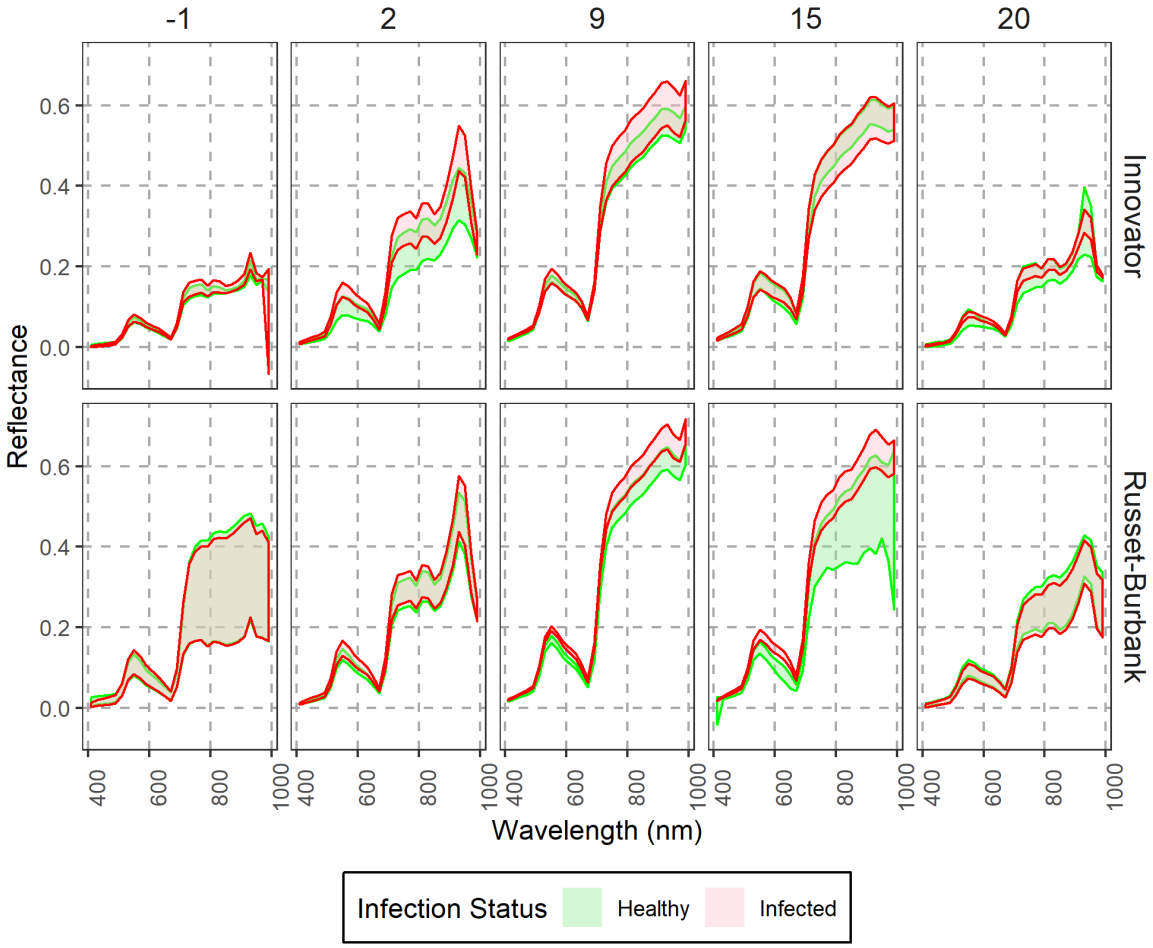

Figure 9. Reflectance spectra of potato plants at five time points since psyllid-mediated CLso infection. The ribbons show the upper and lower bounds of the 90% confidence interval. The numbers at the top of the panels denote the number of days since the plants were exposed to the disease.

We observed the evolution of small but systematic differences in the spectra between infected and healthy plants (Figure 9). These differences evolved over the first 20 days, where for both varieties spectral were indistinguishable before infection. Before infection (Day -1) the spectra overlapped moderately closely for both varieties. Over the ensuing 10 days, the reflectance of plants increased markedly, particularly in the NIR. However, the rate of increase in reflectance was greater for the infected plants and by day 2 the confidence bands for healthy and infected plants had almost separated for the Innovator cultivar in the visible region at 550 nm.

By day 9 a full separation of the confidence bands had occurred across the regions 530-610 nm in the Russet-Burbank cultivar. A partial separation also occurred in the range 730-910 nm in the Russet-Burbank cultivar on this day.

By day 15, the reflectance spectra almost fully overlapped for Innovator and was partially overlapping for Russet-Burbank cultivars.

By day 20, the plants were undergoing heat-induced senescence, spectral reflectance was lower than the previous three measurements and the confidence bands for healthy and infected treatments were largely overlapping.

While the separation of the infected and non-infected confidence bands is only partial, they are consistent with the idea that plant stress elicits greater reflectance in the visible region (Carter, 1993). Since this greater reflectance is systematically associated with infected plants, this seems a reasonable basis to form an early screening system for CLso in the field with an inexpensive camera.

6 Conclusions

Hyperspectral imaging of CLso-infected and uninfected potatoes revealed two possible approaches for early-stage detection of CLso symptoms.

- Each approach required, first, that the living tissue of plants be recognised and separated from the background by converting the hyperspectral imagery to an NDVI image and only including pixels where NDVI exceeded a threshold value of 0.5.
- At 30 days following planting, plants infected with CLso via infected mother tubers had significantly lower leaf area that fell within the NDVI range 0.8 to 0.9 compared with uninfected plants.
- A large proportion of early state psyllid-transmitted CLso-infected plants could be detected within two days following infection (95 days after planting) by searching for anomalously high reflectance in the 570-650 nm in Innovator cultivar and at nine days (105 days following planting) in the Russet-Burbank cultivar.
- Since the differences between infected and healthy plants persist across a wide range of wavelengths, there is a reasonable prospect that a moderately-priced multispectral sensor (rather than an expensive hyperspectral sensor) could be flown by a drone over a potato crop and used to detect individual plants with the disease at an early stage.

7 Recommendations

The findings from this shadehouse study indicated that there is a basis for spectral sensing of CLso-infected plants in a commercial potato crop setting. The next step is to determine whether individual CLso-infected potatoes can be detected using these approaches in the context of commercial potato crop. We recommend the following approach:

- Using a multispectral sensor mounted on a multirotor drone obtain imagery from a potato crop that is known to contain both CLso-infected and healthy plants. Imagery should be acquired at several early time points during the growing season.
- A suitable multispectral sensor might be the popular MicaSense RedEdge MX (MicaSense Inc, Seattle, WA, USA), which acquires imagery in five spectral

bands: three visible (475 nm, 565 nm, 680 nm), the red edge (730) and NIR (840 nm). This retails for $5500 USD.

- Convert multispectral imagery to NDVI and attempt to use object-based image analysis software to segment individual plants into coherent objects.
- For each plant calculate the following metrics:
  - i The amount of leaf area (inferred from number of pixels) within five NDVI classes;
  - ii the median reflectance in the sensors green band.
- Investigate the statistics of these metrics and relate it to the known infection status of potato plants in the imaged area of the crop. The work conducted in this study indicates that: (a) plants infected via the mother tuber will have lower leaf area in the NDVI range 0.8 to 0.9, and (b) that plants infected via the potato psyllid will be more reflective in the 565 nm range. Individual plants that fall into the lower and higher quantiles for metrics (i) and (ii) above, respectively, should be tested for the presense of CLso infection.

8 Acknowledgements

Falk Kalamorz and Lisa Watkins grew the plants, managed the psyllid infection and prepared the shadehouse as a staging site for the experiment. Kishor Kumar constructed and programmed the gantry camera slider system. Paul Peterson provided technical support with the testing of the camera and the gantry. John Hunt and Scott Graham collected the imagery on the fifteen sampling occasions for Experiment 1 and 2. We are grateful to Potatoes NZ for funding this research via an MPI Sustainable Farming Fund Project.

9 References

Carter, G.A., 1993. Responses of Leaf Spectral Reflectance to Plant Stress. American Journal of Botany 80, 239-243.

Carter, G.A., Knapp, A.K., 2001. Leaf optical properties in higher plants: linking spectral characteristics to stress and chlorophyll concentration. American Journal of Botany 88, 677-684.

Filella, I., Penuelas, J., 1994. The red edge position and shape as indicators of plant chlorophyll content, biomass and hydric status. International Journal of Remote Sensing 15, 1459-1470.

Lowe, A., Harrison, N., French, A.P., 2017. Hyperspectral image analysis techniques for the detection and classification of the early onset of plant disease and stress. Plant Methods 13, 80.

Mishra, P., Asaari, M.S.M., Herrero-Langreo, A., Lohumi, S., Diezma, B., Scheunders, P., 2017. Close range hyperspectral imaging of plants: A review. Biosystems Engineering 164, 49-67.

Pitman, A.R., Drayton, G.M., Kraberger, S.J., Genet, R.A., Scott, I.A.W., 2011. Tuber transmission of 'Candidatus Liberibacter solanacearum' and its association with zebra chip on potato in New Zealand. European Journal of Plant Pathology 129, 389-398.

Polder, G., Blok, P.M., de Villiers, H.A.C., van der Wolf, J.M., Kamp, J., 2019. Potato Virus Y Detection in Seed Potatoes Using Deep Learning on Hyperspectral Images. Frontiers in Plant Science 10.

Tucker, C.J., 1979. Red and photographic infrared linear combination for monitoring vegetation. Remote Sesning of the Environment 8, 127-150.

Vereijssen, J., George, M., Kalamorz, F., Dellow, S., Watkins, L., Addison, S., 2019. SFF Precision Agriculture in Seed Potatoes - Year 2 progress report. Plant and Food Research.

Zhao, Z., Prager, S.M., Cruzado, R.K., Liang, X., Cooper, W.R., Hu, G., Rashed, A., 2018. Characterizing Zebra Chip Symptom Severity and Identifying Spectral Signatures Associated with 'Candidatus Liberibacter solanacearum'-Infected Potato Tubers. American Journal of Potato Research 95, 584-596.

Appendix 1 –

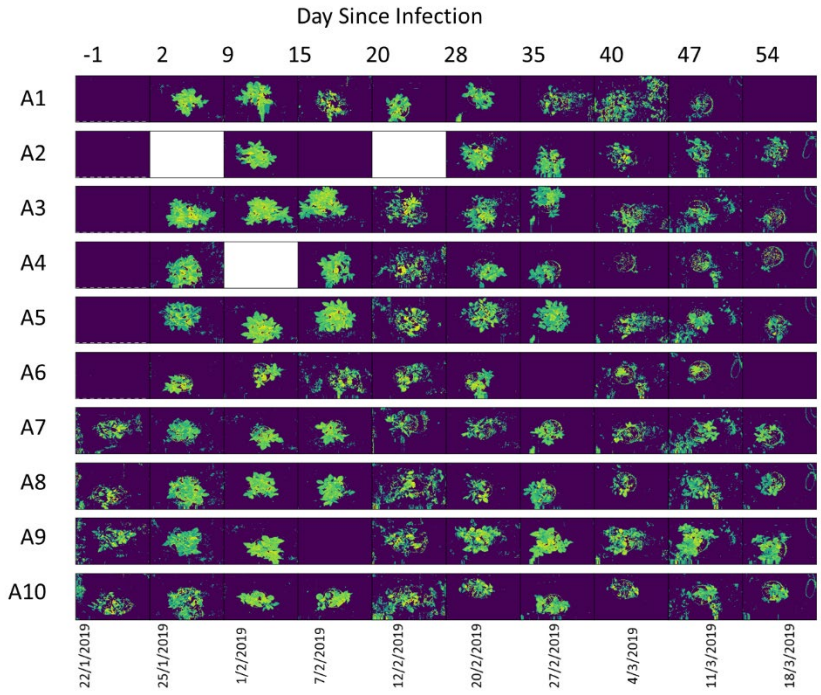

Figure 10 NDVI Images for Experiment 2 — Treatment A: Cultivar "Russet-Burbank" – Not Infected (control). Numbers at top of figure indicate days since infection.

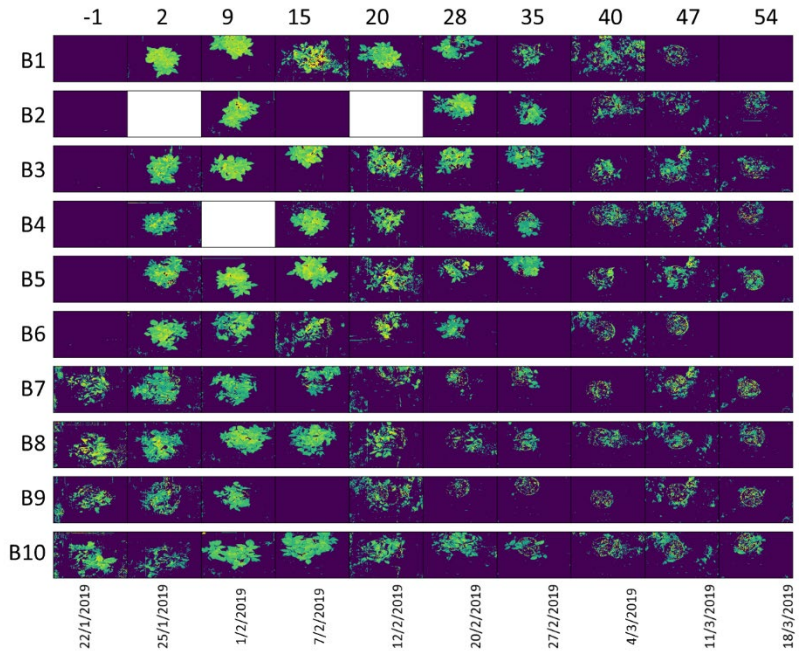

Figure 11 NDVI Images for Experiment 2 — Treatment B: Cultivar "Russet-Burbank" – Infected. Numbers at top of figure indicate days since infection.

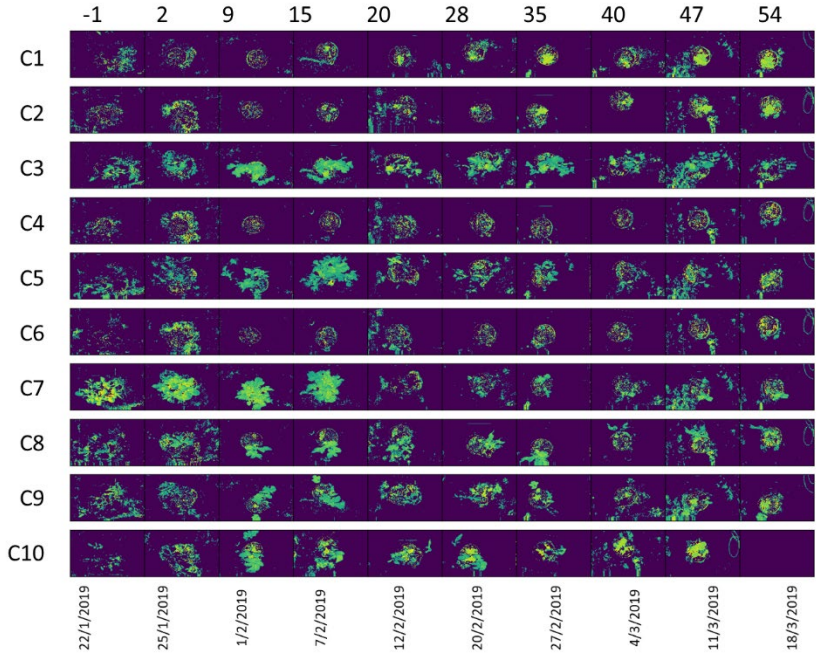

Figure 12 NDVI Images for Experiment 2 — Treatment D: Cultivar "Innovator" – Not Infected. Numbers at top of figure indicate days since infection.

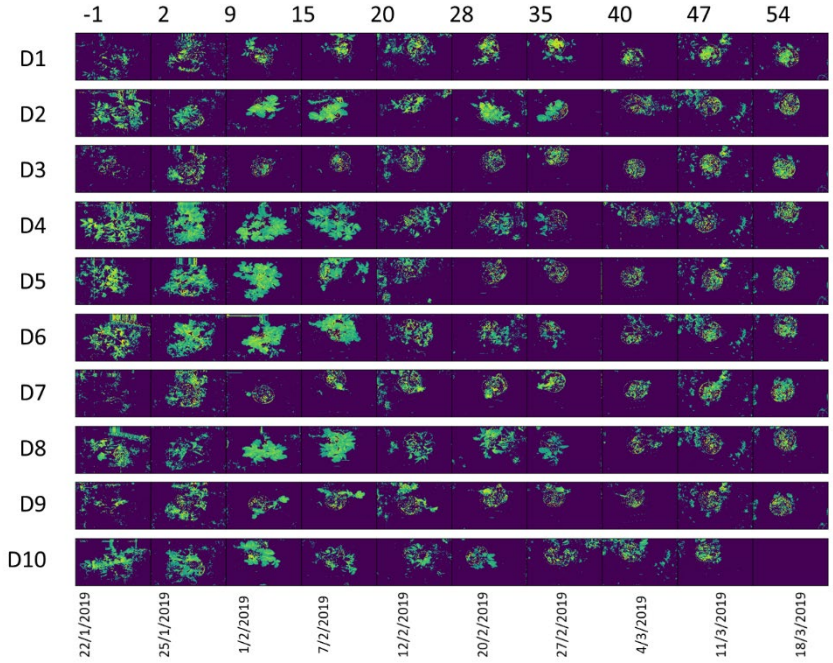

Figure 13 NDVI Images for Experiment 2 — Treatment D: Cultivar "Innovator" – Infected. Numbers at top of figure indicate days since infection.

Plant & Food RESEARCH
RANGAHAU AHUMĀRA KAI

PFR SPTS No. 18039

SFF Improving the quality of seed potatoes using precision agriculture — Year 2 progress report

Vereijssen J, George M, Kalamorz F, Dellow S, Watkins L, Addison S

June 2019

Confidential report for:
Potatoes New Zealand Incorporated

PUBLICATION DATA

Vereijssen J, George M, Kalamorz F, Dellow S, Watkins L, Addison S. June 2019. SFF Improving the quality of seed potatoes using precision agriculture — Year 2 progress report. A Plant & Food Research report prepared for: Potatoes New Zealand Incorporated. Milestone No. 81586: 5&6. Contract No. 36913. Job code: P/336076/01. SPTS No. 18039.

Report approved by:

Jessica Dohmen-Vereijssen
Scientist/Researcher, Insect Behaviour & Ecology
June 2019

Libby Burgess
Science Group Leader, Applied Entomology – Bioprotection
June 2019

CONTENTS

EXECUTIVE SUMMARY

SFF Improving the quality of seed potatoes using precision agriculture — Year 2 progress report

Vereijssen J, George M, Kalamorz F, Dellow S, Watkins L, Addison S
Plant & Food Research Lincoln

June 2019

This research was conducted as part of Milestones 5 and 6 in the second year of SFF 405335 'Improving the quality of seed potatoes using precision agriculture', led by Potatoes New Zealand Incorporated (PNZ). The tomato potato psyllid (*Bactericera cockerelli* (Šulc); Hemiptera: Triozidae) can vector the plant pathogenic bacteria *Candidatus* Liberibacter solanacearum (CLso). CLso is the putative causal agent for zebra chip disease (ZC) in potato, which causes problems for all end-users of the potato industry in New Zealand. (Spectral) imaging in the field is used in this SFF programme to detect CLso or virus-infected plants early in the season, so sources of inoculum can be dealt with before CLso or virus start to spread in the potato field.

Studies in the first year of this SFF using an unmanned aerial vehicle (UAV) with a red/green/blue (RGB) camera in a potato field to detect CLso and virus-infected plants were not successful. In this second year a hyperspectral camera was used on potted plants in a greenhouse. In this second year, a UAV was used to detect re-greening.

The aims of the trials were to:

1. Establish a hyperspectral finger print of potato plants grown from CLso-infected mother tubers to aid detection of CLso-infected potato plants in a seed crop early in the season (a collaboration between Manaaki Whenua - Landcare Research (MWLR) and Plant & Food Research (PFR)
2. Establish a hyperspectral fingerprint of potato plants infected by CLso-positive *B. cockerelli* to aid detection of CLso-infected potato plants in a seed crop early in the season (a collaboration between MWLR and PFR)
3. Detect re-greening in the crop with a UAV, so growers can reduce time and costs spent on desiccation.

Hyperspectral finger printing of potato plants grown from CLso-infected mother tubers

Methods are described in this report, but MWLR will report results in a separate report.

Hyperspectral finger printing of potato plants infected by CLso-positive *B. cockerelli*

Methods are described in this report, but MWLR will report results in a separate report.

Detect re-greening in the crop

Fiji (a software distribution of ImageJ) was used to analyse the UAV images. A custom script was developed to count the number of green pixels in a selected area, which would give an indication of the amount of green plant material present at each visit. Green pixels were then turned red as a visual check to make sure no plant material was missed in the analysis. Re-greening was only observed in the fourth and fifth field visit; the number of plants within the measurement areas was manually counted from the orthomosaics using the count function in Fiji. Unfortunately, the different desiccation treatments as advised by PNZ and applied by the grower did not result in any differences between the three treatments.

For further information please contact:

Jessica Dohmen-Vereijssen
Plant & Food Research Lincoln
Private Bag 4704
Christchurch Mail Centre
Christchurch 8140
NEW ZEALAND

Tel: +64 3 977 7340
DDI: +64 3 325 9566
Fax: +64 3 325 2074
Email: Jessica.Dohmen-Vereijssen@plantandfood.co.nz

1 INTRODUCTION

The plant pathogenic bacteria *Candidatus* Liberibacter solanacearum (CLso) is the putative causal agent for zebra chip disease (ZC) in potato tubers (*Solanum tuberosum* L.) (Abad et al. 2009; Liefting et al. 2009a; Liefting et al. 2009b). The bacterium is vectored by the tomato potato psyllid (*Bactericera cockerelli* (Šulc); Hemiptera: Triozidae) (Secor et al. 2009).

It is important for the seed potato industry to provide clean, un-infected potato seed to the process and fresh market growers and industry. Seed potato growers try to keep their crops free of CLso and aphid-vectored viruses by spraying insecticides. Despite weekly spray regimes, protection against the insect vectors is not completely effective, and foliar and tuber symptoms as a result of virus or CLso can still be seen in crops. Seed crop inspectors rogue (remove) diseased-looking plants, and the tolerance for foliar CLso symptoms was established at 1 in 500 plants in August 2016 (Potatoes New Zealand 2018). Early detection of CLso-infected plants in the field may lead to earlier intervention, a reduced source of CLso in a field, and hopefully fewer ZC-infected tubers being sold as seed.

There are two sources of CLso in a crop: 1. infected mother tubers; and 2. infected *B. cockerelli*. The following characteristics have been observed with respect to mother tubers infected with CLso: a. do not germinate; b. germinate but grow many spindly plants; c. germinate and grow a non-diseased plant; or d. germinate and grow a diseased plant (and subsequently infected daughter tubers) (Pitman et al. 2011).The symptoms these diseased plants show can look quite different from plants infected with CLso by *B. cockerelli* during the season.

After application of a desiccant, some tubers still develop new green shoots either because of ineffective desiccation method or because of the tubers still being quite vigorous; and this is called ‘re-greening’ in this report. If the re-greening is on a large scale, the actively growing green stems and leaves can interfere with machinery when the tubers are mechanically harvested, and the green leaves provide a feeding place for *B. cockerelli*. In the latter case, the seed crop may have been kept fairly free of *B. cockerelli* during the season, which may have resulted in low incidence of ZC, but this can be undone by CLso transmission during re-greening. The disease symptoms as a result of this late infection will develop further in storage.

In the SFF ‘Improving the quality of seed potatoes using precision agriculture’, the focus is on 1. early detection of CLso-infected plants in a seed crop; 2. formulating a desiccation method that reduces re-growth; and 3. detection of re-greening in the crop so growers can reduce time and costs spent on desiccation.

This report is divided into three sections to address early detection of CLso-infected plants and detect re-greening: 1. hyperspectral finger printing of plants grown from CLso-infected mother tubers; 2. hyperspectral finger printing of plants infected by CLso-positive *B. cockerelli*; and 3. detection of re-greening.

2 HYPERSPECTRAL FINGERPRINTING OF POTATO PLANTS GROWN FROM CLSO-INFECTED MOTHER TUBERS

2.1 Materials and Methods

Ten CLso-infected and 10 uninfected potato tubers (*Solanum tuberosum* Moonlight) were obtained from a previous field trial and stored for 6 months at room temperature before planting. The "uninfected/infected" status of each tuber was confirmed using qPCR (Beard & Scott 2013) before planting (data not presented).

On 1 October 2018, each tuber was planted 10 cm deep in a 4-L plastic pot in standard non-sterile potting mix filled 4 cm from the top at Plant & Food Research (PFR) Lincoln. Pots were moved to a shade house, where a tray was placed underneath each pot to act as a water reservoir and to assist even watering between pots. Tubers were watered thoroughly after planting and then once or twice weekly depending on their requirements.

In the shadehouse, RGB (red, green blue colour model) pictures of plants were taken with a Sony Cybershot DSLR camera, using automatic white balance and equalization with GIMP 2.8.8 to spread the colours evenly across the range of possible intensities, which may bring out contrasts that are very difficult to obtain in any other way (i.e. early infection with CLso).

Hyperspectral scanning in a glasshouse to minimise disturbance by wind started on 21 November, conducted by Manaaki Whenua - Landcare Research (MWLR). All plants were scanned every seven days in the same indoor setting in daylight using an automatic rail system which moved the camera at 1 m/s straight above the plants. Two plants (one infected, one uninfected) were documented at the same time, using a reflective panel for subsequent normalisation of data.

2.2 Results

All plants emerged within 3 weeks after planting, with a clear delay for the infected plants in comparison to the uninfected plants (Figure 1). Five weeks after planting the differences were less pronounced (Figure 2).

No differences between infected and uninfected plants were seen in the pictures taken with the Sony Cybershot DSLR camera.

Figure 1. Potato plant grown from an uninfected Moonlight tuber (left) and an infected tuber (right) three weeks after planting (23 October 2018). RGB pictures taken with a Sony Cybershot DSLR, automatic white balance and equalization with GIMP 2.8.8.

Figure 2. Potato plant grown from an uninfected Moonlight tuber (left) and an infected tuber (right) five weeks after planting (5 November 2018). RGB pictures taken with a Sony Cybershot DSLR, automatic white balance and equalization with GIMP 2.8.8.

MWLR will report results in a separate report.

2.3 Discussion

MWLR will discuss results in a separate report.

3 HYPERSPECTRAL FINGERPRINTING OF POTATO PLANTS INFECTED BY CLSO-POSITIVE *B. COCKERELLI*

3.1 Materials and methods

Twenty tubers each of potato 'Russet Burbank' and 'Innovator' were tested for presence of CLso via qPCR (Beard & Scott 2013). All tested negative for CLso (data not presented).

On 19 November 2018, each tuber was planted 10 cm deep in a 4-L plastic pot in standard non-sterile potting mix filled 4 cm from the top at PFR Lincoln. Pots were moved to a shade house, where a tray was placed underneath each pot to act as a water reservoir and to assist even watering between pots. Tubers were watered thoroughly after planting and then once or twice weekly depending on their requirements.

On 23 January, nine weeks after planting, one leaf on 10 plants of each cultivar was exposed to CLso-positive *B. cockerelli*. The adding of the psyllids was delayed by 10-14 days because of non-availability of the hyperspectral camera. A mesh organza bag (Manufacturer MegaView Science) was placed over a leaf of a plant, and vial containing 5 psyllids was carefully placed in the bag (Figure 3). The psyllids were on the plant for 2 weeks, and during this time the potato plants were scanned with a hyperspectral camera. The leaf with the organza bag was removed from the plant on 5 February 2019. Then, a tuber sample of each plant was tested for presence of CLso using qPCR according to Beard & Scott (2013).

Figure 3. Mesh organza bags with vial containing five *Bactericera cockerelli* placed over the leaf of a potted potato plant.

3.2 Results

Plants emerged within 2 weeks after planting and all looked healthy (Figure 4). The dry hot weather was very hard on the potted potato plants, and severe yellowing of leaves was observed (Figure 5).

Figure 4. Potted potato plants 'Russet Burbank' (top) and 'Innovator' (bottom) on 18 December 2018.

All negative plants tested negative for CLso (Appendix A). Two out of 10 infected 'Russet Burbank' tested negative for CLso (tubers D03 and D05), and all 'Innovator' tested positive, indicating the infection process was successful.

MWLR will report results in a separate report.

Figure 5. Yellowing caused by the dry and hot weather in potato 'Russet Burbank' (top) and 'Innovator' (bottom) on 23 January 2019.

3.3 Discussion

MWLR will discuss results in a separate report.

4 DETECTION OF RE-GREENING

4.1 Materials and methods

4.1.1 Paddock, crop and treatment information

The paddock chosen for this trial was on a farmer's property in Valetta, Canterbury (GPS -43.755359, 171.509188).

Potato tubers 'Agria' were planted on 20 December 2018 with a planted population of 70,000 tubers/ha. The potatoes were planted in a bed formation, with three rows making up a bed 1.84 m wide (between wheel centres).

The paddock was approximately 30 ha in size. A 0.9-ha area was intensively monitored with a Trimble Greenseeker crop sensing system (Trimble Agriculture Division, Colorado, USA) and a DJI Phantom 3 Professional UAV (DJI, Shenzhen, China) to provide digital images for downstream image analysis.

The treatment structure (Table 1) aimed to test the optimum application rate of Reglone® (active ingredient 200 g/L Diquat) (Syngenta, New Zealand), a non-selective herbicide for use as a desiccant in crops such as barley, clover and potatoes. Treatments and trial layout were defined by PNZ. For simplicity, any further reference to the rates will be described as 2L, 3L and 4L for treatments 1-3 respectively.

The label rate recommendation depends on the density of the haulms (leaves and stems). For moderate to sparse haulms, a single application of 3 to 4 L in 600 to 1100 L of water/ha is suggested. For dense haulms, two applications seven to ten days apart are recommended with the first application of 3 to 4 L/ha with 600 to 1100 L of water/ha, and the second of 1.5 to 3 L/ha 600 to 1100 L of water/ha (Sygenta New Zealand 2015).

Table 1. Treatment structure for the potato re-greening 2019 trial. The herbicide Reglone® was used for all treatments.

Treatment number	Reglone Spray#1 Applied 11 March	Reglone Spray#2 Applied 18 March	Reglone Spray#3 Applied 24 April
Treatment 1 (2L+2L+2L)	2 L/ha	2 L/ha	2 L/ha
Treatment 2 (2L+3L+3L)	2 L/ha	3 L/ha	3 L/ha
Treatment 3 (2L+4L+4L)	2 L/ha	4 L/ha	4 L/ha

Figure 6 shows a trial plan of the site. Each treatment strip was one spray boom wide x the length of the paddock (24 x ~480 m). The results in this report come from a monitored area between two spans of the lateral irrigator (110 m).

A total of six visits occurred to the trial site, one prior to the first Reglone application (19 February 2019) and five return trips during and after the subsequent two Reglone applications ending 1 May 2019. For each visit, Greenseeker measurements and UAV images were taken.

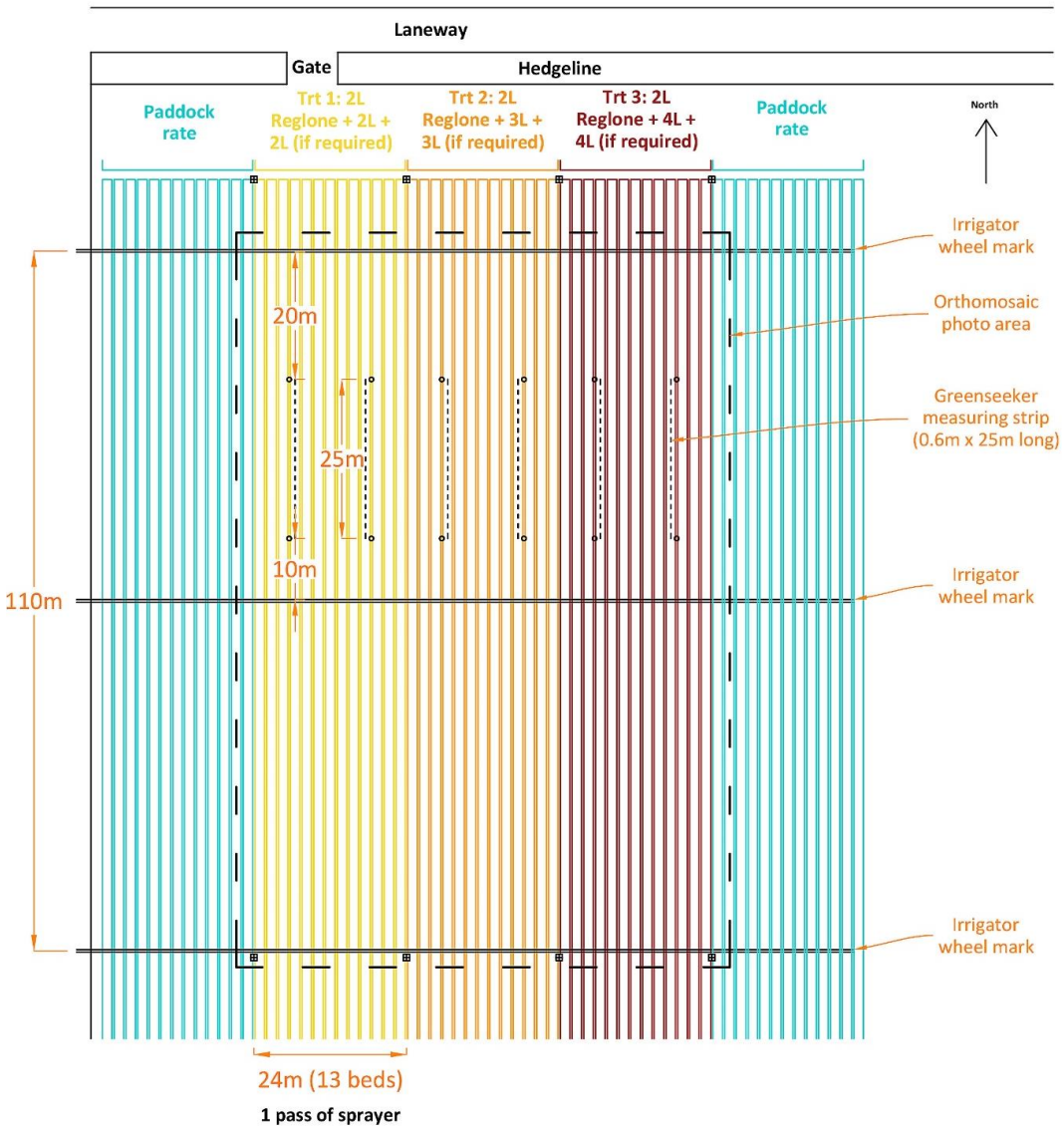

Figure 6. Trial plan for the potato re-greening trial 2019.

4.1.2 Normalised difference vegetation index (NDVI)

Green canopy cover data were collected using the Trimble Greenseeker crop sensing system. The Greenseeker unit is a handheld module designed to be raised approximately 800 mm above the top of a crop canopy. A light source produces light in the visible (red, 660 nanometre) and near-infrared (NIR, 770 nanometre) wavelengths and a sensor measures the amount of reflectance of these wavelengths from the canopy and ground which is recorded at 10 readings per second to a Trimble Recon handheld computer.

At each visit, for each treatment, two ~0.6 x 25 m strips were measured with the sensor placed over the middle potato row of the three row beds. Measurements on return visits were always taken over the same areas. Approximately 180 measurements were recorded for each 25 m strip, providing a total of 360 measurements for each treatment, from which the average reflectance values were calculated.

Reflectance values were converted into a normalised difference vegetation index (NDVI) which can be used as a surrogate for canopy cover (Carlson & Ripley 1997). Reflectance values are influenced by the amount and colour of soil and unwanted plant material. To account for this, extra readings were taken on either bare soil areas (first three visits) or areas with bare soil and dead potato stems (last three visits). A corrected NDVI value was calculated using a scaled NDVI formula: $(NDVI - NDVI_o)/ (NDVI_s - NDVI_o)$ (Carlson & Ripley 1997) where $NDVI_o$ and $NDVI_s$ correspond to the values of NDVI for bare soil or bare soil and dead stems, and a surface with a fractional canopy cover of 100%, respectively.

4.1.3 Digital imagery

With each visit the UAV was flown ~22 m above ground level using the Map Pilot app (https://www.mapsmadeeasy.com/) installed on the UAV iPad. Digital images were taken at this height to achieve a resolution of 1 pixel = 1 cm ground area.

For each visit, approximately 260 digital images were taken and converted into a single high resolution orthomosaic image by Dronescape (Woolston, Christchurch, New Zealand), a Canterbury UAV aerial and analytics company. Each orthomosaic had image dimensions of approximately 12000 x 15000 pixels.

If the UAV was flown at sufficient height to capture the measurement area with one image, the resolution would have only been 1 pixel = 3 cm ground area. In this instance, three times the detail was achieved with an orthomosaic.

4.1.4 Image analysis

Fiji, a software distribution of ImageJ (Schindelin et al. 2012), was used to analyse the images. A custom script was developed by Peter McAtee (PFR) to count the number of green pixels in a selected area, which would give an indication of the amount of green plant material present at each visit. Green pixels were then turned red as a visual check to make sure no plant material was missed in the analysis. For the fourth and fifth visits where re-greening was observed, the numbers of plants within the measurement areas were manually counted from the orthomosaics using the count function in Fiji.

For each treatment, two rectangular regions between irrigator wheel marks were selected, each approximately 1000 m^2 and green pixels were counted (Figure 7).

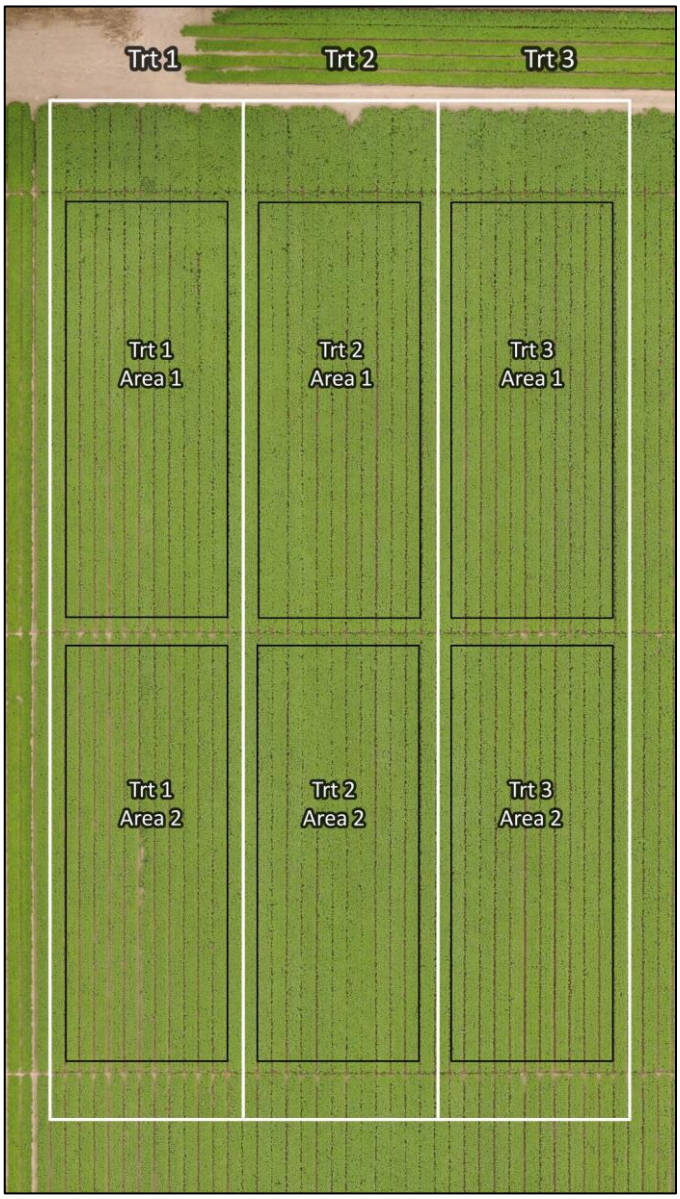

Figure 7. Screenshot from ImageJ showing defined areas (black rectangles) for image analysis. Trt = Reglone® treatment (details in Table 1).

4.2 Results

4.2.1 NDVI

Figure 8 shows the effect of the Reglone treatments on the scaled NDVI values over time. The vertical dashed lines indicate the dates when Reglone was applied.

The second set of data points circled in red (10 March 2019) are an estimate of sensible scaled NDVI values. No actual measurements were recorded on that date, but the canopy would have changed little since the first measurement on 19 February. Without these estimated values, the graph lines would have showed a steady decrease from ~1.0 to ~0.6 but in reality this would not have been the case. Instead there was a sudden drop in green canopy due to the first Reglone

application on 11 March. This approach of inserting estimated data is also used for the data generated from the image analysis.

There was virtually no difference between 2L, 3L and 4L Reglone treatments, with all three showing a sharp decrease in scaled NDVI values over time once the Reglone applications occurred. At visits four and five, re-greening was observed in all three treatments. It was however, minimal and there was no noticeable rise in NDVI values for any of the three treatments.

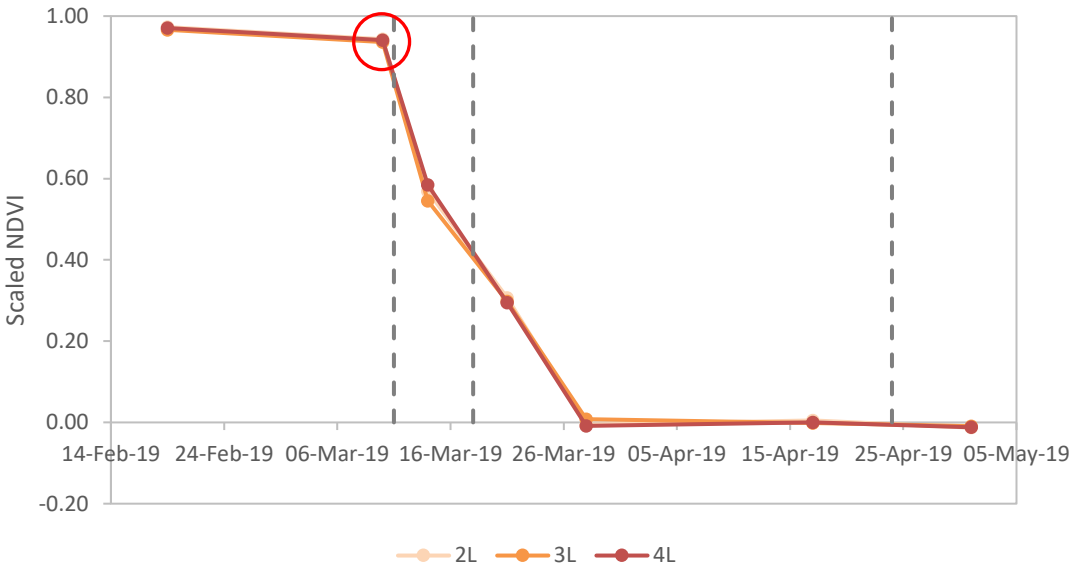

Figure 8. Scaled normalised difference vegetation index over the 2019 season to measure reflectance of potato 'Agria'. Points within the red circle indicate estimated values. Crop canopy would have still been close to full cover prior to the first Reglone® application, but no measurements were taken immediately before the first spray. 2L, 3L and 4L refer to the Reglone treatments; refer to Table 1 for treatment details.

4.2.2 Image analysis

Using image analysis, the decline in green canopy cover due to the Reglone applications was calculated from the change in percentage of green pixels in the image analysis areas (Figure 9). The trend for all three treatments were very similar to each other, and similar to the scaled NDVI data (Appendix B). Regardless of Reglone rate, Reglone applications steadily decreased the percentage of green pixels in the orthomosaics.

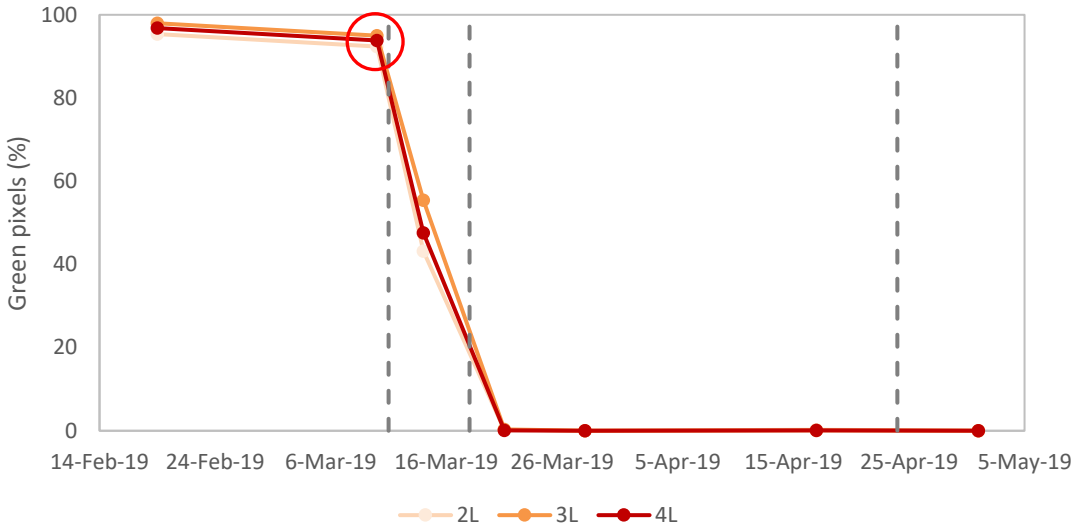

Figure 9. Change in green potato canopy cover due to the Reglone® treatments depicted by the percentage of green pixels measured in the orthomosaics. Vertical dashed lines indicate Reglone applications. The points within the red circle indicate estimated values. Crop canopy would have still been close to full cover prior to the first Reglone application, but no measurements were taken immediately before the first spray. 2L, 3L and 4L refer to the Reglone treatments; refer to Table 1 for treatment details.

4.2.3 Re-greening plant counts

For visits four (28 March) and five (17 April), re-greening was observed in the measurement area (Figure 10).

Using the Cell Counter plugin in Fiji, the numbers of plants with fresh regrowth since the second spray were manually counted (Table 2).

Figure 10. Cropped image from orthomosaic taken on 17 April 2019. The two red circles indicate where re-greening of potato plants occurred.

On 17 April, the highest rate of Reglone (Treatment 3) appeared to have more re-greening than the other two treatments. However, it is important to note that these counts were performed on approximately 2000 m^2 of potato beds containing approximately 14,000 potato plants. Whether there were 35 or 26 plants showing re-greening, the actual percentage of total plants is virtually the same (0.25% and 0.19% respectively).

Table 2. Occurrence of re-greened potato plants within each treatment area on the fourth and fifth visits. Results taken from visual inspection of the orthomosaics.

Date	Treatment 1	Treatment 2	Treatment 3
28-Mar-19	10	5	6
17-Apr-19	26	27	35

4.3 Discussion

The results show that in this paddock it was probably irrelevant which Reglone treatment was used, given that all three treatments appeared to affect the potato plants to the same degree.

For all treatments, there was a sharp decline of about 50% green canopy cover after the first Reglone application, with a steady decline in canopy cover over time after subsequent spray events. Approximately 8-10 days after the second application, regardless of Reglone rate, the

green canopy cover was essentially 0% and further time was required only for the dead stems to soften and decay.

This result was somewhat surprising, but Reglone is used at very different rates to desiccate potato haulms depending on grower experience, density of haulms, and weather. The Reglone rate the grower used over the rest of the paddock was very effective, more so than the grower had ever seen before (Potato grower, pers. comm., 3 April 2019).

There may have been a greater divergence in the results if the treatments had no similarities in rate across the treatments and the water rate used. For example, for the first application, if a high rate of Reglone was used in conjunction with a high water rate, the active ingredient may have penetrated deeper into the plant canopy, causing more desiccation than traditional chemical and water rates.

Re-greening was first observed within the treatment areas 10 days after the second Reglone application, and was easy to count with close examination of the orthomosaic images. The use of orthomosaics and image analysis allowed a large area of the crop to be examined, and green canopy cover could be quantified free of human bias. This procedure had minimal time commitment compared with traditional field inspections, and with some minor adjustments (flying lower, with less overlap between images), more detailed orthomosaics should be achievable.

Future experiments should look at the interactions of cultivar and timing of Reglone application, which have been known to cause problematic re-greening in the past. However, because the EPA is intending to reassess paraquat and diquat, and given the fate of these active ingredients overseas, researching other methods for potato haulm desiccation or destruction should have priority.

5 REFERENCES

Abad JA, Bandla M, French-Monar RD, Liefting LW, Clover GRG 2009. First report of the detection of *'Candidatus* Liberibacter' species in Zebra Chip disease-infected potato plants in the United States. Plant Disease 93: 108-109.

Beard SS, Scott IAW 2013. A rapid method for the detection and quantification of the vector-borne bacterium '*Candidatus* Liberibacter solanacearum' in the tomato potato psyllid, *Bactericera cockerelli*. Entomologia Experimentalis et Applicata 147: 196-200.

Carlson TN, Ripley DA 1997. On the relation between NDVI, fractional vegetation cover, and leaf area index. Remote Sensing of Environment, 62: 241-252.

Liefting LW, Weir BS, Pennycook SR, Clover GR 2009a. '*Candidatus* Liberibacter solanacearum', associated with plants in the family Solanaceae. International Journal of Systematic and Evolutionary Microbiology 59(Pt 9): 2274-2276.

Liefting LW, Sutherland PW, Ward LI, Paice KL, Weir BS, Clover GRG 2009b. A new '*Candidatus* Liberibacter' species associated with diseases of Solanaceous crops. Plant Disease 93: 208-214.

Maps Made Easy. (2019). Map Pilot. Retrieved from https://www.mapsmadeeasy.com/

Potatoes New Zealand 2018. New Zealand Seed Potato Certification Authority 2018-2019 Rulebook. Seed potato Certification Scheme and 2018 Certified Seedlines. 25 October 2018. Potatoes New Zealand Inc. 54 pp.

Pitman AR, Drayton GM, Kraberger SJ, Genet RA, Scott IAW 2011. Tuber transmission of '*Candidatus* Liberibacter solanacearum' and its association with zebra chip on potato in New Zealand. European Journal of Plant Pathology 129: 389-398.

Schindelin J, Arganda-Carreras I, Frise E, Kaynig V, Longair M, Pietzsch T, Preibisch S, Rueden C, Saalfeld S, Schmid B, Tinevez JY 2012. Fiji: an open-source platform for biological-image analysis. Nature Methods 9: 676-682.

Secor GA, Rivera VV, Abad JA, Lee IM, Clover GRG, Liefting LW, Li X, De Boer SH 2009. Association of '*Candidatus* Liberibacter solanacearum' with zebra chip disease of potato established by graft and psyllid transmission, electron microscopy, and PCR. Plant Disease 93: 574-583.

Syngenta New Zealand 2018. Reglone. Retrieved from https://www.syngenta.co.nz/product/crop-protection/herbicide/reglone. Accessed 7 June 2019.

APPENDIX A. DETAILS OF QUANTITATIVE POLYMERASE CHAIN REACTION (QPCR) ON TWO VARIETIES OF POTATO TO DETECT *CANDIDATUS* LIBERIBACTER SOLANACEARUM (CLSO)

	Variety	Status	Sample ID	Sample Tissue	Extraction date	qPCR date	Ct[1] 1 (Clso)	Copy number 1 (Clso)	Ct 2 (Clso)	Copy number 2 (Clso)	Ct 3 (Clso)	Copy number 3 (Clso)	Ct 1 (plant)	Copy number 1 (plant)	CT 2 (plant)	Copy number 2 (plant)	Ct 3 (plant)	Copy number 3 (plant)
1	Innovator	healthy	A01	Daughter Tuber	190529	190530							16.72	1.05E+07	16.73	1.04E+07	16.72	1.05E+07
2	Innovator	healthy	A02	Daughter Tuber	190529	190530							17.20	7.68E+06	17.21	7.62E+06	17.25	7.42E+06
3	Innovator	healthy	A03	Daughter Tuber	190529	190530							15.09	3.01E+07	15.53	2.27E+07	15.54	2.25E+07
4	Innovator	healthy	A04	Daughter Tuber	190529	190530							15.44	2.41E+07	15.41	2.45E+07	15.45	2.40E+07
5	Innovator	healthy	A05	Daughter Tuber	190529	190530							15.64	2.11E+07	15.66	2.08E+07	15.64	2.11E+07
6	Innovator	healthy	A06	Daughter Tuber	190529	190530							16.64	1.10E+07	16.58	1.15E+07	16.39	1.30E+07
7	Innovator	healthy	A07	Daughter Tuber	190529	190530							15.43	2.42E+07	15.35	2.55E+07	15.34	2.57E+07
8	Innovator	healthy	A08	Daughter Tuber	190529	190530							16.69	1.07E+07	16.75	1.03E+07	16.72	1.05E+07
9	Innovator	healthy	A09	Daughter Tuber	190529	190530							15.13	2.93E+07	15.09	3.01E+07	14.87	3.48E+07
10	Innovator	healthy	A10	Daughter Tuber	190529	190530							16.09	1.58E+07	16.07	1.60E+07	16.10	1.56E+07
11	Innovator	infected	B01	Daughter Tuber	190529	190530	26.16	17210	26.18	16990	25.95	19780	15.11	2.98E+07	14.99	3.22E+07	15.00	3.20E+07
12	Innovator	infected	B02	Daughter Tuber	190529	190530	25	38340	25.08	36310	25.15	34530	14.27	5.12E+07	14.27	5.13E+07	14.24	5.23E+07
13	Innovator	infected	B03	Daughter Tuber	190529	190530	25.05	36830	25.03	37580	25.1	35600	14.61	4.13E+07	14.63	4.05E+07	14.59	4.17E+07
14	Innovator	infected	B04	Daughter Tuber	190529	190530	28.81	2747	28.84	2694	28.88	2622	16.53	1.19E+07	16.75	1.03E+07	16.72	1.05E+07
15	Innovator	infected	B05	Daughter Tuber	190529	190530	25.41	28830	25.3	31070	25.45	27950	14.72	3.82E+07	14.66	3.97E+07	14.72	3.83E+07
16	Innovator	infected	B06	Daughter Tuber	190529	190530	26.53	13250	26.5	13620	26.67	12040	14.46	4.54E+07	14.46	4.54E+07	14.41	4.67E+07
17	Innovator	infected	B07	Daughter Tuber	190529	190530	23.74	91040	23.77	89140	23.66	96700	14.13	5.61E+07	14.16	5.52E+07	14.07	5.85E+07
18	Innovator	infected	B08	Daughter Tuber	190529	190530	24.36	59390	24.44	56130	24.47	54970	14.41	4.69E+07	14.46	4.55E+07	14.51	4.38E+07
19	Innovator	infected	B09	Daughter Tuber	190529	190530	24.68	47640	24.71	46850	24.78	44390	14.26	5.17E+07	14.01	6.07E+07	14.36	4.85E+07
20	Innovator	infected	B10	Daughter Tuber	190531	190603	24.82	37870	24.88	36240	24.84	37130	13.76	1.14E+08	13.68	1.21E+08	13.75	1.16E+08
21	Russet Burbank	healthy	C01	Daughter Tuber	190529	190530							15.20	2.90E+07	15.26	2.78E+07	15.10	3.09E+07
22	Russet Burbank	healthy	C02	Daughter Tuber	190529	190530							15.70	2.11E+07	15.62	2.22E+07	15.55	2.31E+07
23	Russet Burbank	healthy	C03	Daughter Tuber	190529	190530							15.12	3.05E+07	15.13	3.04E+07	15.05	3.20E+07
24	Russet Burbank	healthy	C04	Daughter Tuber	190529	190530							14.76	3.84E+07	14.80	3.74E+07	14.82	3.71E+07
25	Russet Burbank	healthy	C05	Daughter Tuber	190529	190530							14.38	4.89E+07	14.46	4.67E+07	14.58	4.31E+07

	Variety	Status	Sample ID	Sample Tissue	Extraction date	qPCR date	Ct[1] 1 (Clso)	Copy number 1 (Clso)	Ct 2 (Clso)	Copy number 2 (Clso)	Ct 3 (Clso)	Copy number 3 (Clso)	Ct 1 (plant)	Copy number 1 (plant)	CT 2 (plant)	Copy number 2 (plant)	Ct 3 (plant)	Copy number 3 (plant)
26	Russet Burbank	healthy	C06	Daughter Tuber	190529	190530							15.81	1.96E+07	15.87	1.89E+07	15.74	2.05E+07
27	Russet Burbank	healthy	C07	Daughter Tuber	190529	190530							17.97	4.90E+06	18.00	4.82E+06	17.93	5.04E+06
28	Russet Burbank	healthy	C08	Daughter Tuber	190529	190530							17.19	8.09E+06	17.14	8.35E+06	17.18	8.13E+06
29	Russet Burbank	healthy	C09	Daughter Tuber	190529	190530							15.01	3.27E+07	15.01	3.28E+07	14.85	3.63E+07
30	Russet Burbank	healthy	C10	Daughter Tuber	190529	190530							15.20	2.89E+07	15.33	2.67E+07	15.19	2.93E+07
31	Russet Burbank	infected	D01	Daughter Tuber	190531	190503	23.88	73020	23.97	68640	23.96	69250	14.11	8.99E+07	14.19	8.49E+07	14.18	8.55E+07
32	Russet Burbank	infected	D02	Daughter Tuber	190529	190530	25.36	26980	25.34	27290	25.24	29210	14.65	4.13E+07	14.63	4.19E+07	14.63	4.17E+07
33	Russet Burbank	infected	D03	Daughter Tuber	190529	190530							15.97	1.77E+07	16.00	1.73E+07	15.99	1.74E+07
34	Russet Burbank	infected	D04	Daughter Tuber	190529	190530	26.03	17340	26.05	17010	25.98	17850	13.79	7.18E+07	13.92	6.58E+07	13.94	6.53E+07
35	Russet Burbank	infected	D05	Daughter Tuber	190529	190530							16.29	1.44E+07	16.27	1.46E+07	16.27	1.46E+07
36	Russet Burbank	infected	D06	Daughter Tuber	190529	190530	25.32	27700	25.22	29720	25.29	28230	16.02	1.71E+07	16.01	1.73E+07	16.02	1.71E+07
37	Russet Burbank	infected	D07	Leaf Tissue	190305	190306	35.88	17.21	35.49	22.86	36.04	15.32	15.99	1.71E+07	16.03	1.67E+07	15.95	1.75E+07
38	Russet Burbank	infected	D08	Daughter Tuber	190529	190530	25.11	31900	25.07	32800	25.16	30900	15.19	2.93E+07	15.26	2.80E+07	15.23	2.85E+07
39	Russet Burbank	infected	D09	Daughter Tuber	190529	190530	24.87	37500	24.69	42090	24.76	40220	15.49	2.41E+07	15.48	2.42E+07	15.53	2.35E+07
40	Russet Burbank	infected	D10	Daughter Tuber	190529	190530	26.73	10830	26.75	10710	26.6	11860	15.35	2.64E+07	15.48	2.42E+07	15.34	2.65E+07

[1]Ct: Cycle threshold of qPCR, is defined as the number of cycles required for the fluorescent signal to cross the threshold (i.e. exceeds background level).

APPENDIX B. RE-GREENING ORTHOMOSAIC IMAGES

The following orthomosaics were generated from each of the six visits. Adobe® Photoshop was used to create the labels and white boundary lines. These orthomosaics have been resized from ~9500x1500 pixels to ~1700x1000 pixels. The original full sized jpgs, tiffs and kmz files are available from Mike George, PFR.


Trt 1
Trt 2
Trt 3
Visit 2. 14-03-2019


Trt 1
Trt 2
Trt 3
Visit 3. 21-03-2019


Trt 1
Trt 2
Trt 3
Visit 4. 28-03-2019

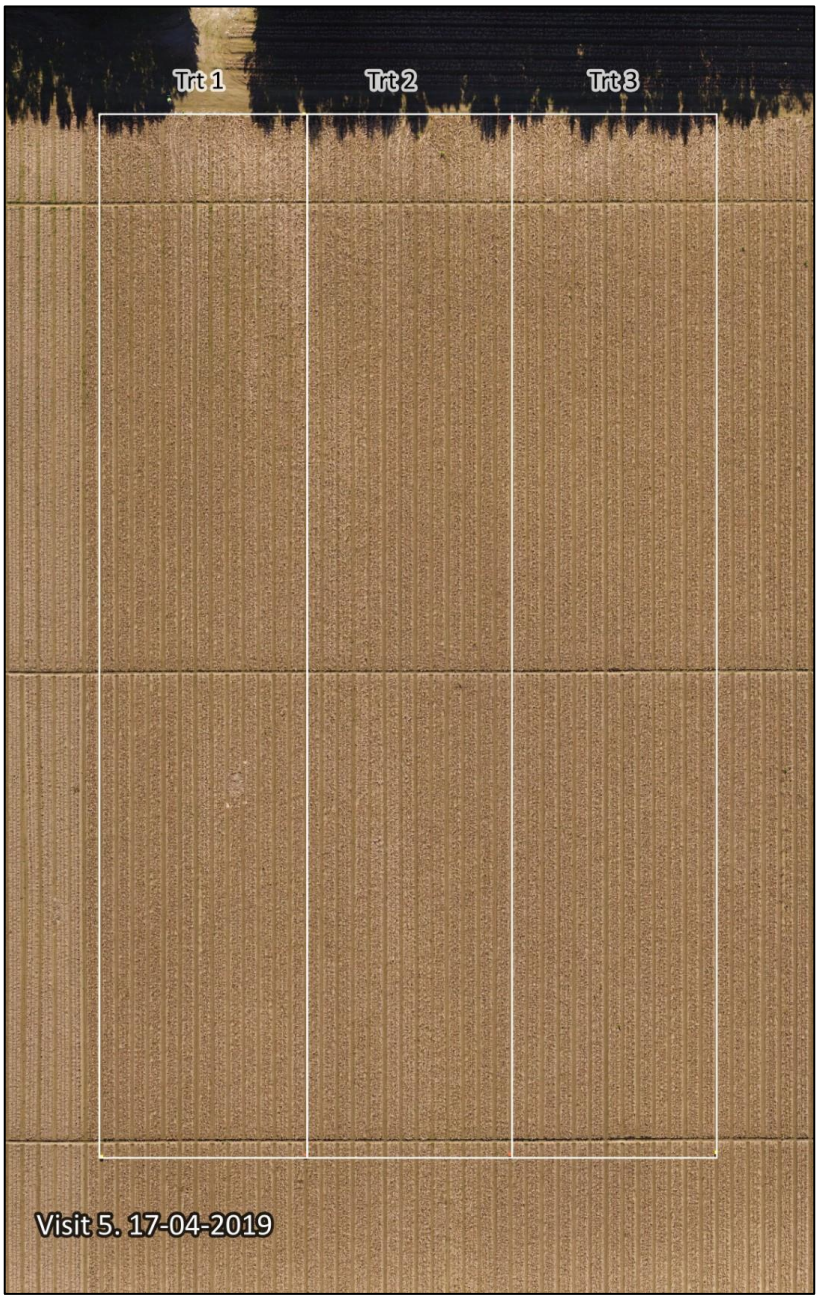
Trt 1
Trt 2
Trt 3
Visit 5. 17-04-2019

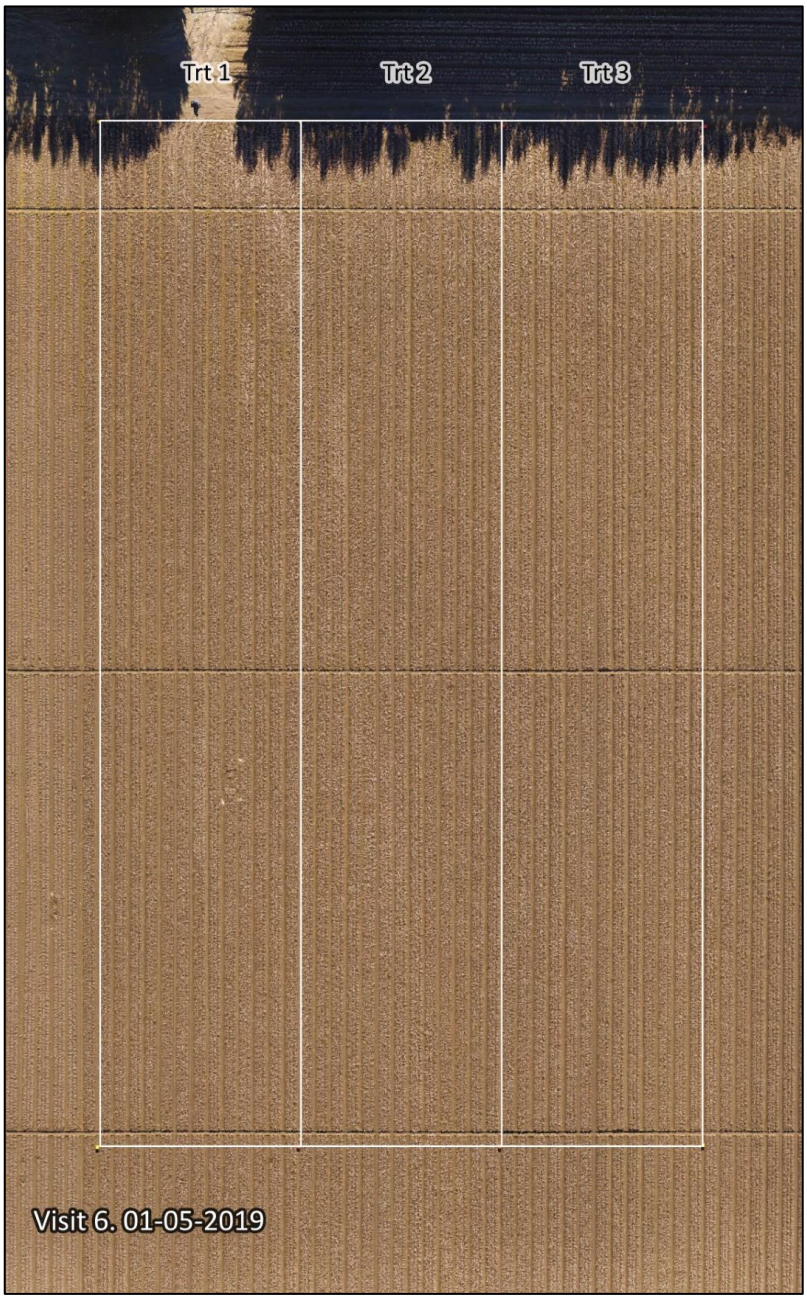
Trt 1
Trt 2
Trt 3
Visit 6. 01-05-2019

DISCOVER. INNOVATE. GROW.

PFR SPTS No. 20955

Detection of "*Candidatus* Liberibacter solanacearum" infection in seed potatoes using multispectral UAV imagery

Jochym M

June 2021

1 Executive summary

"Candidatus Liberibacter solanacearum" (Lso) is the bacterium causing zebra chip disease in potatoes. Seeds obtained from potato plants are a potential vector for the spread of Lso; it is therefore important to rapidly identify Lso-positive areas in fields of seed potatoes pre-harvest.

Multispectral drone imagery may prove as a useful tool in detection of Lso infection in seed potato fields. Multispectral drone images contain the information on the amount of light reflected by plants; reflectance is measured at least five light wavelengths: blue (475 nm), green (560 nm), red (668 nm), red edge (717 nm), and near infrared (840 nm). Reflectance values are routinely used to calculate various indices of plant health (e.g. Normalised Differential Vegetation Index).

There exists a possibility that Lso-positive and -negative plants will have a specific multispectral signature. The existence of such signature should be established in a future greenhouse experiment. If it is found, a predictive model of Lso infection in potato fields could be built. Such model could rapidly identify areas with Lso infection in multispectral drone images of potato fields, and inform harvest operations to prevent its spread. This project, conducted by The New Zealand Institute for Plant and Food Research Limited (PFR), explores the initial steps towards prediction of Lso in multispectral drone images and identifies remaining work.

2 Project objectives

The aim of this project was to explore the potential of multispectral aerial imagery as a tool for the detection of areas of seed potato fields infected with Lso. For this purpose, Potatoes New Zealand Incorporated (PNZ) supplied a number of datasets collected with an Unmanned Aerial Vehicle (UAV) along with field infection data ('ground truth'). PFR processed the multispectral aerial data into multispectral orthophotos (reflectance maps), and matched them with ground truth data. Finally, we made recommendations for further steps towards a predictive model of Lso infection in fields of potato plants.

We identified the following objectives for this project:

1. Assessment of the completeness and quality of available aerial data
2. Generation of georeferenced multispectral orthophotos
3. Assessment of available ground truth data; matching ground truth data with multispectral orthophotos
4. Identification of a signature of Lso infection in multispectral data (contingent upon successful completion of Objective 3)
5. Prediction of Lso infection in fields of potato plants with the use of aerial multispectral imagery (contingent upon successful completion of Objective 4)
6. Recommendations.

3 Objective 1: Assessment of the aerial data

The data supplied by PNZ were collected by a third party using a UAV-mounted MicaSense RedEdge M multispectral camera; this camera model collects images in five bands: blue (B), green (G), red (R), near infrared (NIR), and red edge (RE). The dimensions of the images were 1280 x 960 pixels.

Multispectral imagery was collected at two sites ('Tinwald' and 'West Farm') on two separate dates (Tinwald: 29 January 2020 and 10 February 2020; West Farm: 15 January 2020 and 10 February 2020). In each instance the data collection missions were flown at three altitudes (20 m, 40 m, and 60 m).

We found that the datasets collected on 29 January 2020 (Tinwald) and 5 January 2020 (West Farm) were incomplete: only complete sets of B images existed, with NIR band images present sporadically, and with isolated images for G, R, and RE bands. This degree of data incompleteness suggests an equipment malfunction or operator error, where the images are taken in too short a succession. Effectively these datasets were eliminated from further processing. Only image sets collected on 10 February 2020 were complete in terms of the number of images in each band (Table 1 contains a summary of data completeness).

Table 1. Numbers of collected images in each band at each site, date, and altitude in metres ('Alt'). Note that in a complete dataset the number of images in each band should be equal.

Site	Date	Alt	B (475 ± 10 nm)	G (560 ± 10 nm)	R (668 ± 5 nm)	RE (717 ± 5 nm)	NIR (840 ± 20 nm)
Tinwald	2020-01-29	20	407	21	0	0	103
Tinwald	2020-01-29	40	90	3	0	0	22
Tinwald	2020-01-29	60	61	5	0	0	20
Tinwald	2020-02-10	20	456	456	456	456	456
Tinwald	2020-02-10	40	91	91	91	91	91
Tinwald	2020-02-10	60	60	60	60	60	60
West Farm	2020-01-15	20	704	16	0	0	105
West Farm	2020-01-15	40	168	3	0	0	24
West Farm	2020-01-15	60	75	2	0	0	10
West Farm	2020-02-10	20	699	699	699	699	699
West Farm	2020-02-10	40	176	176	176	176	176

Using the information embedded within the Exchangeable Image File (EXIF) of the complete datasets, we established the metrics of the UAV data collection missions (Table 2).

Table 2. Unmanned Aerial Vehicle (UAV) mission metrics for complete datasets: average altitude, distance flown, number of captures (each consisting of a set of images, one in each of the five bands), mission duration, average speed, and average distance separating consecutive captures ('separation').

Site	Altitude (m)	Distance flown (m)	N	Duration (s)	Average speed (m/s)	Average speed (km/h)	Separation (m)	Separation (s)
Tinwald	20	1555	456	595	2.61	9.4	3.4	1.30
Tinwald	40	618	91	130	4.75	17.1	6.8	1.43
Tinwald	60	620	60	100	6.20	22.3	10.3	1.67
West Farm	20	2389	699	890	2.68	9.6	3.4	1.27
West Farm	40	1209	176	231	5.23	18.8	6.9	1.31
West Farm	60	795	75	113	7.04	25.3	10.6	1.51

We identified issues with the complete datasets which were likely to increase the error of the resulting reflectance information. The longitudinal overlap of the datasets was estimated at 60–70%; there was a possibility of the image overlap being insufficient for the orthophoto generation, especially that image overlap is reduced further in data processing because of clipping after band alignment. Additionally, images with low overlap may result in artefacts in features above ground level, or may make the generation of orthophotos altogether impossible. Further, we found significant motion blur present in multiple images (Figure 1); the missions were flown at a high speed (Table 2), with a too slow (automatic) shutter speed setting. Motion blur has a negative impact on the resolution of the final orthophoto and the quality of the reflectance data for downstream analysis. The multispectral camera was set to automatic exposure, adding to inconsistency within the datasets (Figure 2). We also found that the lighting conditions were variable during the data collection missions, which adds further variability to the data.

Figure 1. Example of an image with significant motion blur.

Figure 2. Example of inconsistency in exposure of consecutive images.

Multispectral imagery datasets require calibration to known values of reflectance; reference values are obtained immediately before and after a data collection mission. In the available data, however, the calibration images were collected only before the first flight, and after the third (Figure 3).

3.1 Conclusions to Objective 1

We found that only half of the datasets were complete. The complete datasets had a number of technical shortcomings resulting from the protocol for data collection: minimal overlap of successive images, excessive flight speed causing motion blur, automatic exposure and slow shutter speed causing uneven exposure throughout dataset and motion blur, and variable lighting conditions. These issues were likely to increase the error of the downstream processing of reflectance data.

We proceeded with the processing of the complete datasets for the Tinwald and West Farm sites.

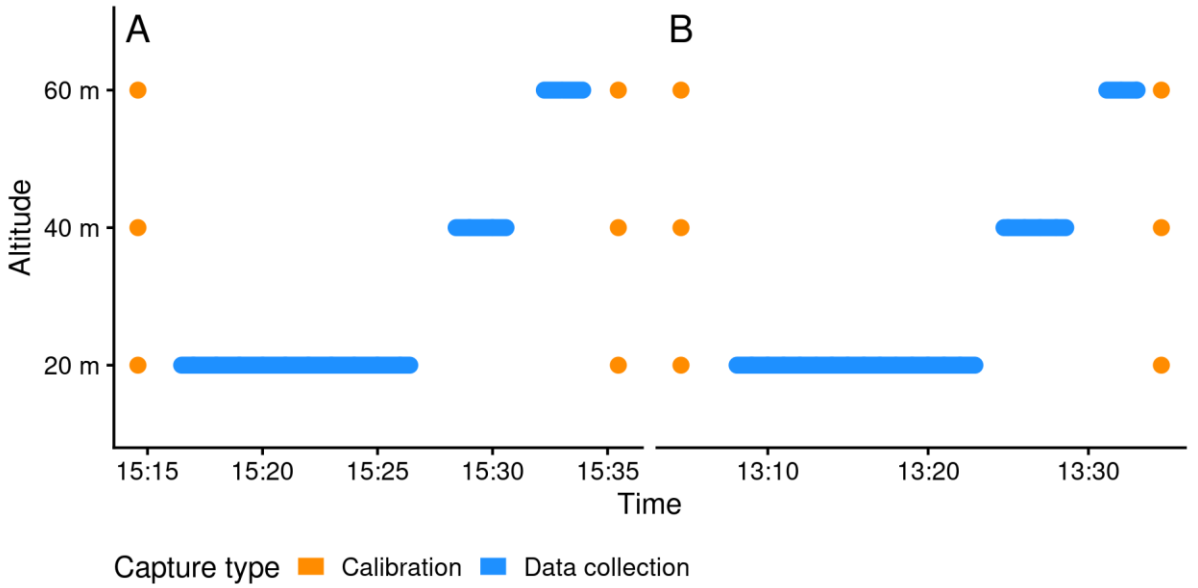

Figure 3. Timing of data collection (blue bars) and calibration captures (orange dots) at Tinwald (A) and West Farm (B).

4 Objective 2: Georeferenced multispectral orthophotos

Identification of a feature (e.g. location of sample) in an aerial image requires that the image be georeferenced, meaning that the area represented in the image corresponds to an area on the ground, which is defined with a set of geographic coordinates. Georeferencing of aerial imagery is obtained by means of ground control points (GCPs). GCPs are features positioned on the ground at accurately defined locations, which are then identified in the images (Figure 4). The datasets supplied by PNZ included a set of GCPs along with matching coordinates. We proceeded by identifying GCPs in raw images and generating an input file containing the information required by the image processing software. Subsequently, we pre-processed the multispectral images by removing vignetting and distortion, and proceeded with a radiometric calibration of the datasets using calibration images (supplied by PNZ; Figure 4) and reflectance values of the calibration panel (obtained from the calibration panel manufacturer). Both of the available captures of the calibration panel (before and after flight) were used in the calibration process. As a result, the digital number (DN) values contained in raw images were converted into reflectance values.

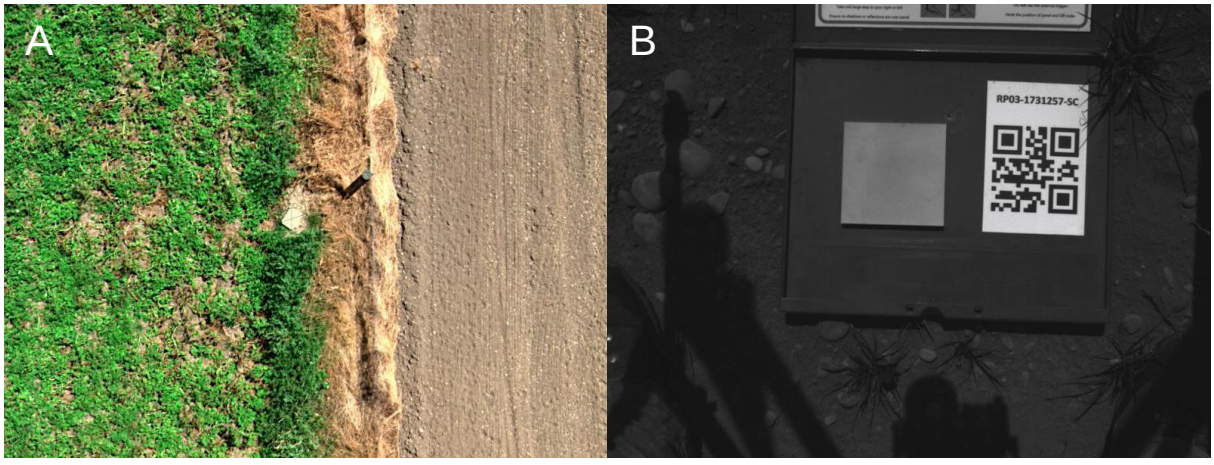

Figure 4. Example of a ground control point (GCP) – white rectangle at centre of image (A). Example of a calibration panel capture in blue band (B).

Multispectral images from the five bands must align so that each pixel in a set of B, R, G NIR, and RE images comprising a single capture represents the same location on the ground. There are multiple ways of obtaining band alignment; we tested the results of band alignment using the *RigRelatives* EXIF tag (a descriptor of the relative positions of the five lenses of the multispectral camera). However, we found that using warp matrices produced a slightly better result and proceeded with this method. The warp matrices were computed individually for each of the six datasets (Table 2). In the final preparatory step, the aligned bands were cropped to a common region and saved to individual monoband images with relevant EXIF information appended.

The generation of georeferenced multiband orthophotos (i.e. reflectance maps; Figures 5 and 6) was accomplished using OpenDroneMap software (version 2.3.0).

Figure 5. True-colour (red, green, blue) miniature of the orthophoto generated for the 'Tinwald' site from imagery acquired at 20 m altitude.

Figure 6. True-colour (red, green, blue) miniature of the orthophoto generated for the 'West Farm' site from imagery acquired at 20 m altitude.

4.1 Conclusions to Objective 2

Datasets collected from an altitude of 20 m produce a satisfactory 5-band orthophoto at a resolution of 1.5 cm to a pixel (see Figures 5 and 6 for RGB miniatures). Combining images from 20 m, 40 m, and 60 m altitude flights produced unacceptable results (blurry patches with varying level of detail); images from 40 m and 60 m missions approached separately might have produced an acceptable result but at estimated resolution of only 3 and 4.5 cm to a pixel, respectively. We deemed the highest available resolution (1.5 cm to a pixel; obtained at altitude of 20 m) as appropriate for subsequent objectives.

5 Objective 3: Assessment of field data

We found that for the 'Tinwald' site, 12 samples of field data fell within the area we have multispectral data for (Figure 7). Of these, only a single sampling point was labelled as 'healthy', two were recorded as showing symptoms of chemical damage, and nine had been identified as infected with zebra chip disease (Table 3).

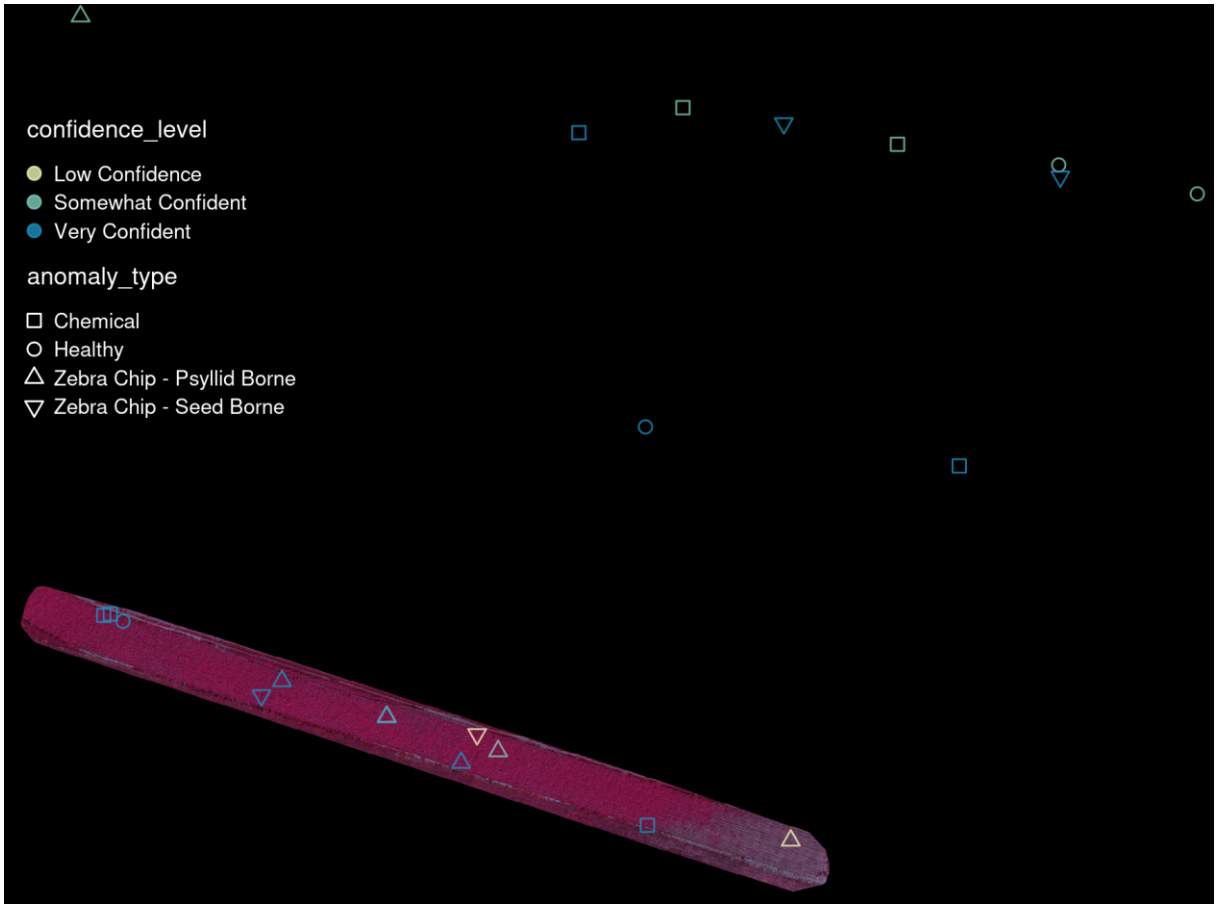

Figure 7. False-colour (near infrared, blue, green) miniature of the orthophoto generated for the 'Tinwald' site from imagery acquired at 20 m altitude. Symbols indicate locations of available samples of healthy plants as well as plants bearing symptoms of disease or chemical damage, both within the area covered by the orthophoto and in surrounding fields (shown in black).

Table 3. Ground truth data for the 'Tinwald' site (supplied by Potatoes New Zealand Incorporated).

Sample ID	Anomaly type	Confidence level
S_20	Chemical	Very confident
S_22	Chemical	Very confident
S_9	Chemical	Very confident
S_8	Healthy	Very confident
S_15	Zebra chip – psyllid borne	Low confidence
S_16	Zebra chip – psyllid borne	Low confidence
S_17	Zebra chip – psyllid borne	Somewhat confident
S_18	Zebra chip – psyllid borne	Very confident
S_19	Zebra chip – psyllid borne	Very confident
S_21	Zebra chip – psyllid borne	Very confident
S_10	Zebra chip – seed borne	Very confident
S_7	Zebra chip – seed borne	Low confidence

No field samples fell within the area covered by the orthophoto at the 'West Farm' site (Figure 8).

5.1 Conclusions to Objective 3

The amount of available data (one negative and eight positive samples; Table 3) is insufficient to build a predictive model of Lso infections in potato plants. This constitutes a negative outcome of Objective 3 (Assessment of available ground truth data). Hence, further objectives of this project cannot proceed.

On the following pages we demonstrate what further steps towards a predictive model would look like, using the multispectral data at hand as an example.

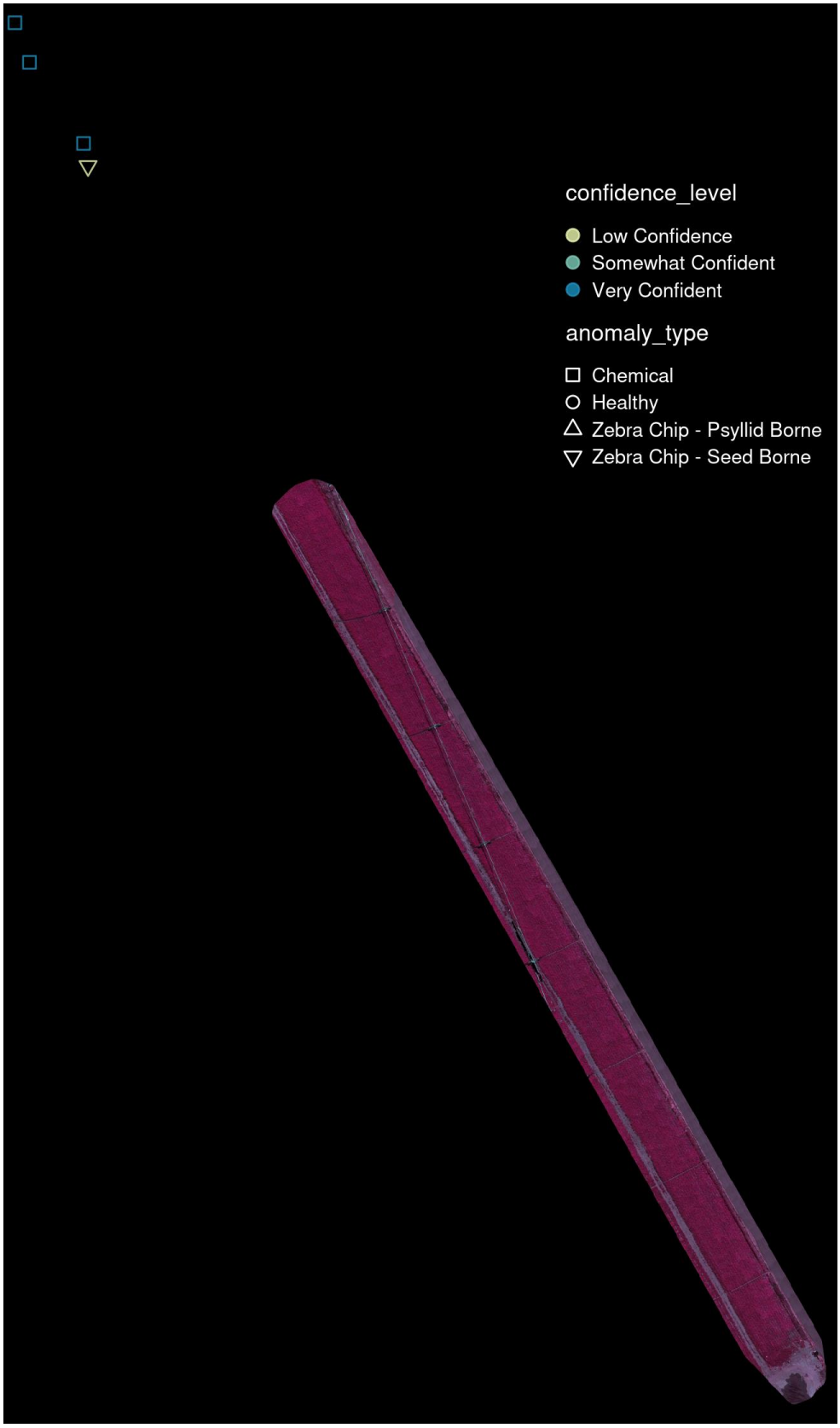

Figure 8. False-colour (near infrared, blue, green) miniature of the orthophoto generated for the 'West Farm' site from imagery acquired at 20 m altitude. Symbols indicate locations of available samples of healthy plants as well as plants bearing symptoms of disease or chemical damage, both within the area covered by the orthophoto and in surrounding fields (black).

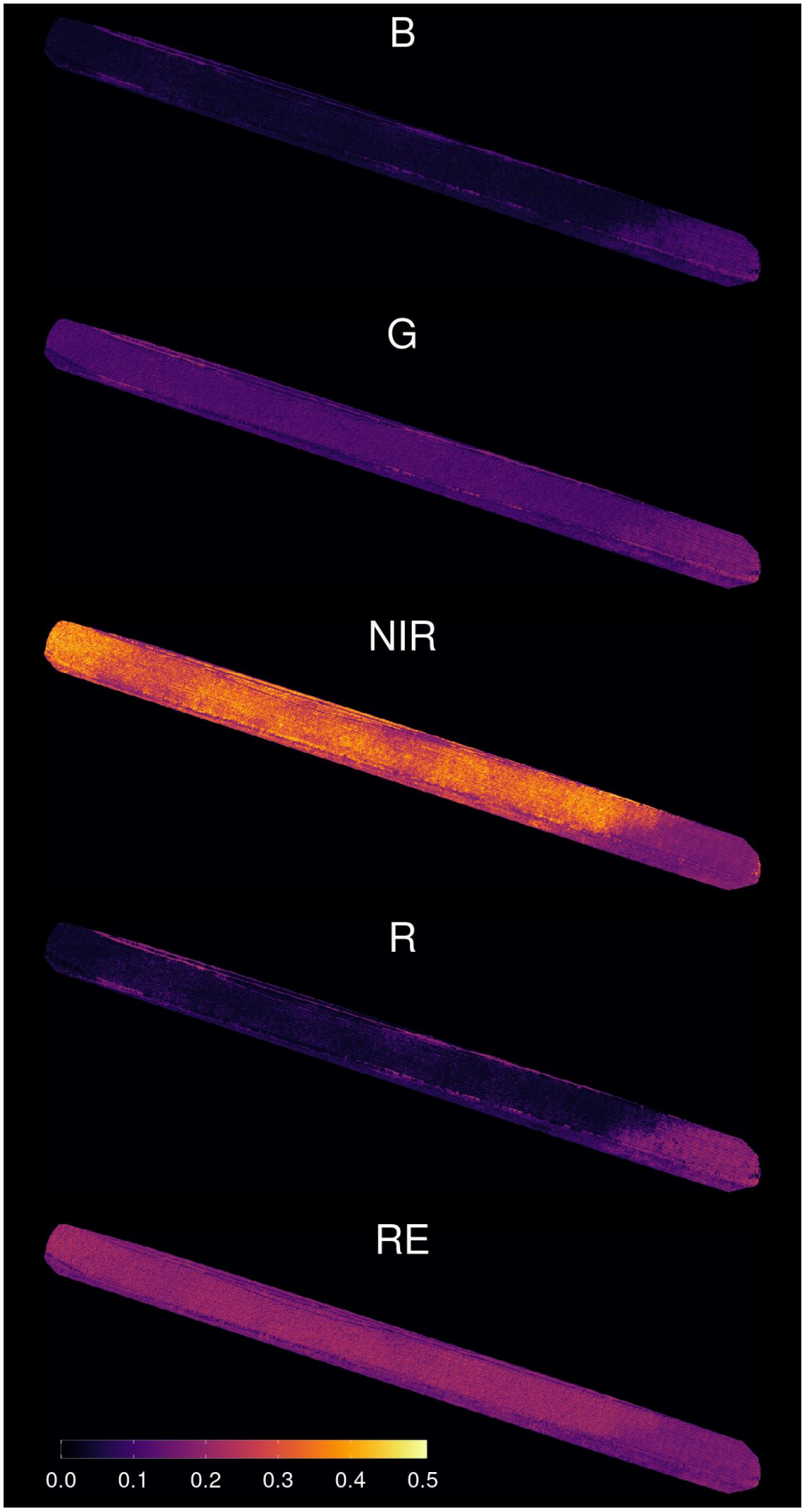

Figure 9. Reflectance values in each of the five bands at the 'Tinwald' site. 0 indicates complete absorption (note high absorption in blue (B) and red (R) bands due to high chlorophyll content), while 1 indicates complete reflectance. G = green; NIR = near infrared; RE = red edge.

6 Plant health indices at sample locations

The georeferenced multispectral orthophotos contain information on reflectance of incident light in five bands (B, G, R NIR, RE; Figure 9). These data can be used to compute various indices of plant health. Two commonly used indicators of plant health are the Normalised Differential Vegetation Index (NDVI) and the Normalised Differential Red Edge (NDRE). NDVI (Figure 10) and NDRE (Figure 11) are calculated using the reflectance values according to the following formulae:

$$NDVI = \frac{(NIR - R)}{(NIR + R)}$$

$$NDRE = \frac{(NIR - RE)}{(NIR + RE)}$$

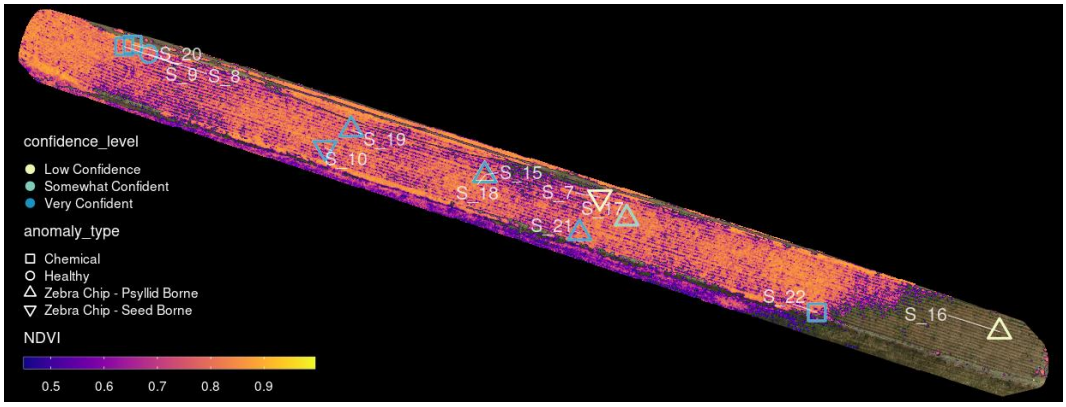

Figure 10. Normalised Differential Vegetation Index (NDVI) values at the 'Tinwald' site, overlaid over a corresponding true colour image (miniature). The following criteria were used in the calculation of NDVI: areas of bare soil and shadow (near-infrared reflectance <0.20) were removed. Index values were limited to plants (cut-offs: >45 percentile; <99.5 percentile NDVI). Symbols indicate locations of the samples.

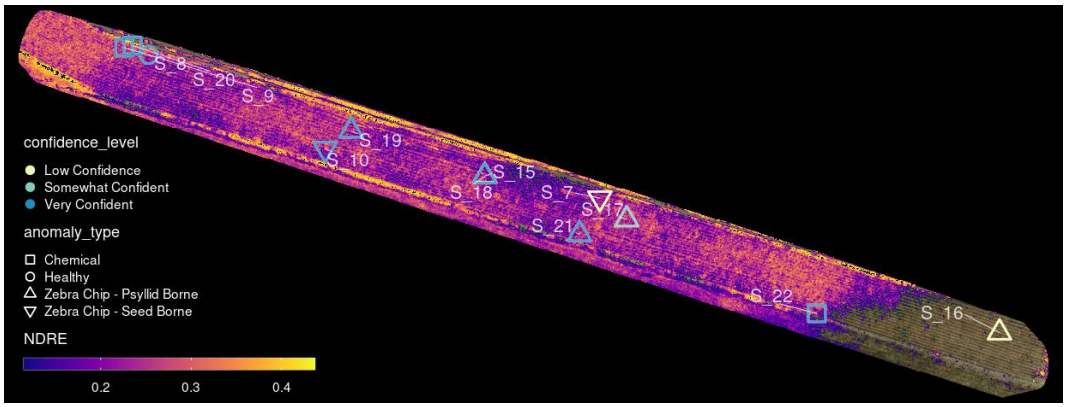

Figure 11. Normalised Differential Red Edge (NDRE) values at the 'Tinwald' site, overlaid over a corresponding true colour image (miniature). The following criteria were used in the calculation of NDRE: areas of bare soil and and shadow (NIR reflectance <0.20) were removed. Index values were limited to plants (cut-offs: >20 percentile; <99.5 percentile NDRE). Symbols indicate locations of the samples.

6.1 Plant health indices at sampled locations

Figures 12 and 13 show values of NDVI and NDRE, respectively, at locations sampled for 'ground truth' data (Table 3). The values are limited to visible plant matter, and cropped to multispectral image pixels within several arbitrary radii of the sample location. Values of NDVI, NDRE, or ideally, an index devised to detect a specific difference in a multispectral signature of Lso-negative and positive plants could serve to build a predictive model of Lso infection in seed potato fields.

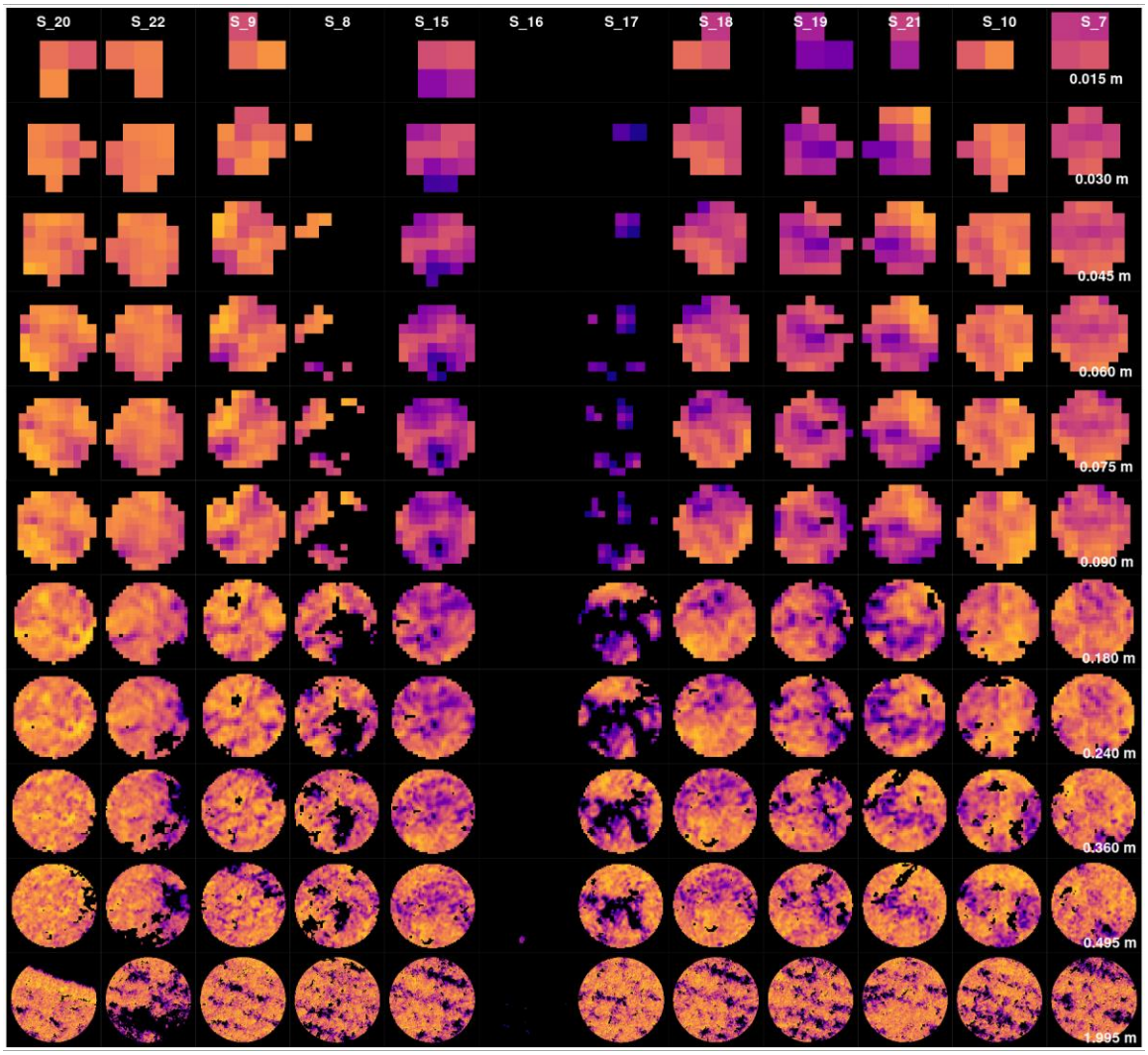

Figure 12. Normalised Differential Vegetation Index (NDVI) values within a 1.5, 3, 4.5, 6, 7.5, 9, 18, 24, 36, 49.5, and 199.5 cm radius of sample location (1, 2, 3, 4, 5, 6, 12, 16, 24, 33, 133 pixels at 1.5 cm/px resolution, respectively). NDVI values were limited to visible plant matter. See Figure 10 for scale.

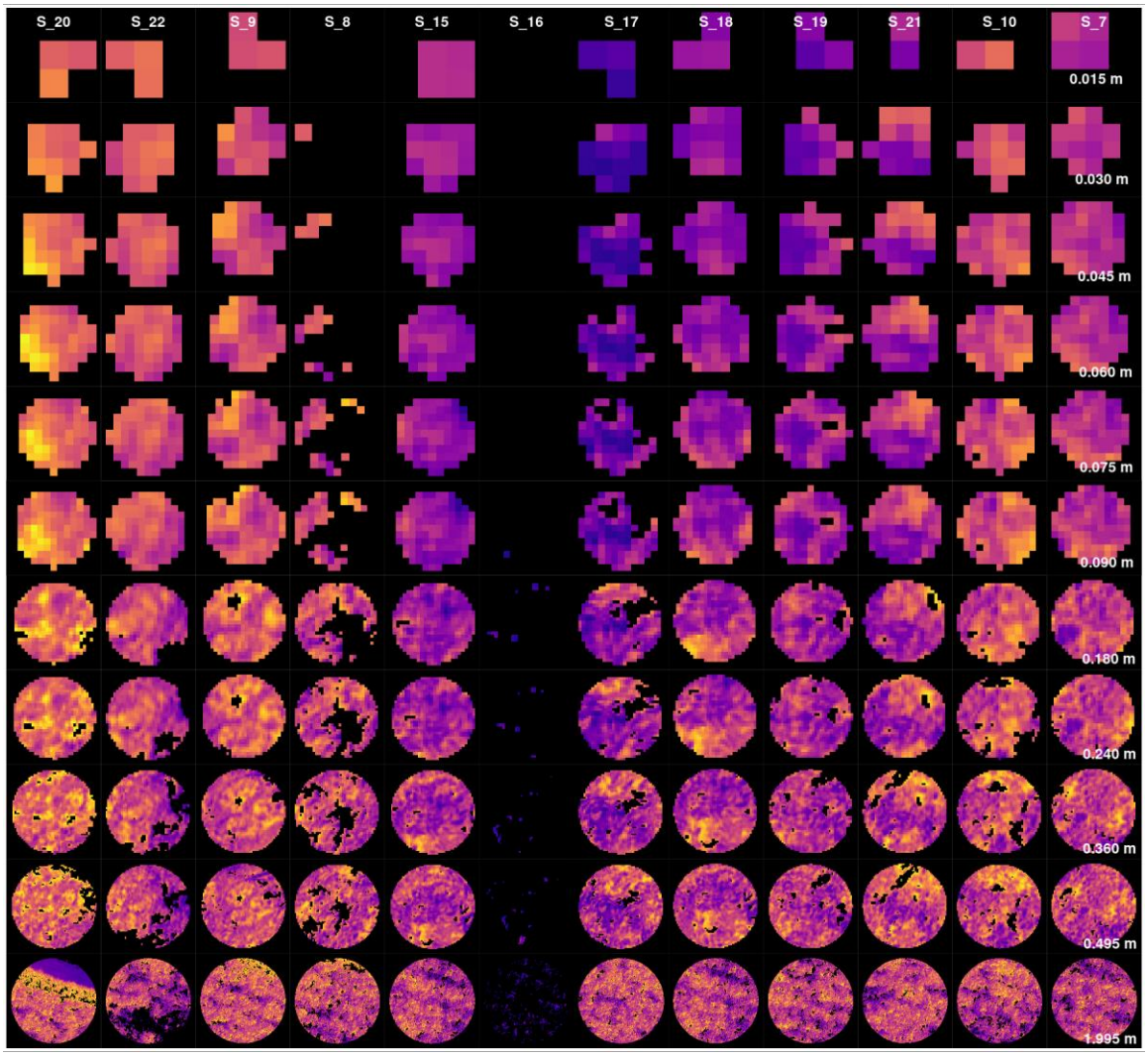

Figure 13. Normalised Differential Red Edge (NDRE) values within a 1.5, 3, 4.5, 6, 7.5, 9, 18, 24, 36, 49.5, and 199.5 cm radius of sample location (1, 2, 3, 4, 5, 6, 12, 16, 24, 33, 133 pixels at 1.5 cm/px resolution, respectively). NDRE values were limited to visible plant matter. See Figure 11 for scale.

7 Recommendations

Certain prerequisites would have to be met for a predictive model of Lso infections in potato fields to be built. NDVI and NDRE, the two plant health indices presented above, are indicators of plant stress; as such, they may not be specific enough to indicate whether a potato plant is infected with Lso or stressed due to other factors (e.g. drought, malnutrition, other diseases).

The key prerequisite is that the multispectral or hyperspectral signature of Lso-positive plants is specific enough to differentiate them from Lso-negative plants. Potentially, multispectral or hyperspectral imagery obtained in a greenhouse setting could be used to identify these signatures. This would require a standalone, dedicated trial. In such trial, the minimum required sample size for both Lso-negative and positive plants would need to be large enough to establish such a difference; the minimum required sample size would depend on the magnitude of the difference in the signatures of Lso-negative and positive plants. The magnitude of this difference would also determine what confidence level the predictive model would have.

Once a specific signature of Lso-positive potato plants is established, a predictive model could be built. Such a model would require 'training' data consisting of a large enough number of Lso-negative and -positive samples. The signatures of individual Lso-negative and -positive plants obtained in a controlled environment might not extrapolate to field conditions because of a number of factors (e.g. overlapping individual plants, variable environmental conditions), so the 'training' data (multispectral or hyperspectral UAV imagery of infected and healthy areas) would have to be obtained experimentally in a dedicated field trial. Such a trial should include designated areas with potato plants deliberately infected with Lso, and areas of plants verified as Lso-negative. Arriving at both the required sample size and the optimal measurement radius (one that maximises the difference between a Lso-positive and negative signal; see Figures 12 & 13 for examples) would require a pilot trial. Further specifics of experimental design of the field trial and the pilot trial would have to be established separately.

Ultimately, an operating predictive model of Lso infection in potato fields would take a georeferenced orthophoto generated for the area of interest as input; the model would identify areas of suspected Lso infection of potato plants with a given confidence level.

The multispectral or hyperspectral reflectance data collected with UAVs will serve both as 'training' data, and as input for the predictive model. We recommend that these data be acquired according to best-practice guidelines for UAV photogrammetry, including a generous overlap between successive images (to allow for overlap reduction during data processing), slow flight speed (to eliminate motion blur), and fixed exposure parameters and stable lighting conditions (to eliminate extrinsic variability in reflectance data). To preserve as much detail as possible, we recommend the lowest practicable altitude for UAV data collection flights.

8 Next steps

- Verification of a Lso-specific multispectral or hyperspectral signature in a greenhouse trial with a range of Lso-positive and negative plants
- 'Training' data pilot trial, to establish minimum required sampling size and an optimal measurement radius around a 'ground truth' sample location
- Collection of multispectral or hyperspectral 'training' data in a field trial with Lso-negative and Lso-positive areas
- Validation of a predictive model of Lso infection in fields of seed potato plants.

Confidential report for:

Potatoes New Zealand Incorporated
PNZ-27 SFF 405335

PUBLICATION DATA

Jochym M. June 2021. Detection of *"Candidatus Liberibacter* solanacearum" infection in seed potatoes using multispectral UAV imagery. A Plant & Food Research report prepared for: Potatoes New Zealand Incorporated. Milestone No. 89631. Contract No. 38946. Job code: P/422502/01. PFR SPTS No. 20955.

Report prepared by:

Mateusz Jochym
Scientist, Pollination Ecology
June 2021

Report approved by:

David Pattemore
Science Group Leader, Productive Biodiversity & Pollination
June 2021

For further information please contact:

Mateusz Jochym
Plant & Food Research Ruakura
Private Bag 3230
Waikato Mail Centre
Hamilton 3240
NEW ZEALAND

Tel: +64 7 959 4430
DDI: +64 7 959 4552
Email: Mateusz.Jochym@plantandfood.co.nz